International Journal of Thermofluids 24 (2024) 100990

Contents lists available at ScienceDirect

International Journal of Thermofluids

journal homepage: www.sciencedirect.com/journal/international-journal-of-thermofluids

CFD modelling of Darcian flow of water in porous media: Effects of sand grain size

Asseel M.Rasheed Al-Gaheeshi [a], Farhan Lafta Rashid [b], Mudhar A. Al-Obaidi [c], Karrar A. Hammoodi [d], Ephraim Bonah Agyekum [e,f,g,h,*]

[a] Department of Electrical and Electronic Engineering, University of Kerbala, Karbala, 56001, Iraq
[b] Department of Petroleum Engineering, College of Engineering/University of Kerbala, Karbala, 56001, Iraq
[c] Institute of Technical Instructor Training, University of Middle Technical University, Baghdad, 10074, Iraq
[d] Conditioning and Refrigeration Department, Engineering, Faculty/University of Warith Al-Anbiyaa, Karbala, 56001, Iraq
[e] Nuclear and Renewable Energy Department, Ural Federal University Named after the First President of Russia, Boris Yeltsin, 19 Mira Street, Ekaterinburg, 620002, Russia
[f] Applied Science Research Center. Applied Science Private University, Amman, Jordan
[g] Jadara University Research Center, Jadara University, Jordan
[h] Tashkent State University of Economics, 100066, Tashkent city, Islam Karimov Street 49, Uzbekistan

ARTICLE INFO

Keywords:
CFD modelling
Darcian flow
Porous media
Grain size

ABSTRACT

This research addresses the challenges of flow dynamics in porous media by utilising Brinkman equations that describe the relationships between fluid dynamics, particle diameter, and inlet velocity. A systematic analysis of these factors is presented, with a focus on pressure gradients, friction factors, and detailed descriptions of flow characteristics under various conditions. The research uses computational fluid dynamics (CFD) to analyse the influence of particle size and inlet velocity on fluid flow through porous media. The Reynolds number is employed to illustrate how large pressure gradients are dependent on flow regimes, with transitional flow indicated by high Reynolds numbers. It was observed that an increase in inlet velocity results in a higher-pressure gradient due to increased resistance within the porous medium. As a consequence, the flow velocity decreases as the fluid progresses through the porous structure, highlighting the interaction between flow resistance and velocity distribution. Additionally, the findings reveal that particle diameter directly influences flow behaviour, with smaller particles causing higher friction factors and steeper pressure gradients at lower velocities. When the inlet velocity increases, the pressure gradient and friction factor improve, reflecting an increase in the fluid's resistance level. This work suggests that future research should explore the effects of fluid properties, such as viscosity and density, as well as the geometric configurations of porous media. The conclusions emphasize the importance of considering particle size and flow conditions in the design of porous media systems. The findings contribute to the understanding of fluid dynamics and the optimal design of porous structures, aiding in the development of more accurate and efficient models for engineering applications.

1. Introduction

In the last few decades, researchers have focused a great deal of emphasis on fluid flow, heat, and mass transfer in porous media. The performance of heat and mass transport in fluids is primarily controlled by the thermo-physical characteristics of the fluid and the characteristics of the porous medium's permeability [1]. Given its wide range of engineering uses, including solidification of casting, ground hydrology, thermal and insulating engineering, ground hydrology, petroleum reservoirs, nuclear waste repositories, pollutant dispersion in aquifers, crystal growth in fluids, and chemical catalytic reactors [2,3], etc.—the number of research studies on this subject has increased. Researchers have utilised the Darcy's law a lot to estimate fluid flow in porous spaces [4]. Darcy's law relates the viscosity of a fluid flowing through a porous medium, with a pressure drop over a certain distance. It is applicable only under steady, Newtonian, incompressible, isothermal, and creeping flow conditions with no slip at the solid-fluid interface, and when

* Corresponding author.
E-mail addresses: asseelmrasheed@uokerbala.edu.iq (A.M.Rasheed Al-Gaheeshi), farhan.lefta@uokerbala.edu.iq (F.L. Rashid), dr.mudhar.alaubedy@mtu.edu.iq (M.A. Al-Obaidi), karrar.al@uowa.edu.iq (K.A. Hammoodi), agyekumephraim@yahoo.com (E.B. Agyekum).

https://doi.org/10.1016/j.ijft.2024.100990

Available online 30 November 2024

Nomenclature

Symbol	Description unit
D	Container diameter m
d	Particle diameter m
f	Friction factor -
L	Container length m
P	Pressure Pa
Re	Reynolds number -
u	Average velocity m/s
x	x component in cartesian direction
y	y component in cartesian direction -
Greek symbols	
ρ	Density kg/m^3
μ	Viscosity Pa s
ϵ	Mean porosity -
κ	Permeability m^2
ΔP	Pressure drops Pa
Subscripts	
p	Particle
pm	Porous medium
x	x component in cartesian direction
y	y component in cartesian direction

inertial effects are negligible [5,6]. Additionally, upscaling approaches such as the method of volume averaging and homogenisation are widely used in the prediction of permeability tensor components in porous media. These methods enable the determination of macroscopic properties by solving the corresponding closure problem, which bridges the gap between microscale and macroscale descriptions of flow behaviour. These techniques are particularly useful in cases where direct simulation or experimental measurements at the microscale are difficult or computationally expensive.

The presence of the medium's frequently erratic solid structure along the fluid's route is the primary cause of the intricacy of fluid movement within porous materials. The flow field is significantly altered by this construction, which eliminates boundary layers and forces the fluid to only move via narrow, tortuous open flow passageways. Strong mixing and the emergence of a new mechanism known as dispersion are caused by these processes. Consequently, compared to open-area flows, the pressure loss in porous medium is substantially larger. The properties of flow patterns in media with pores, the energy dissipation mechanisms within each regime, and the transition between regimes are prerequisite knowledge for comprehending the pressure-drop penalty. Fluid flow in porous media has been extensively studied [7–12] due to its significance in both artificial and natural settings.

A particle-packed medium's particle diameter is one of the most important fundamental components of the pore structure. This is used to characterise the pore geometry features together with the gradation, grain form, and surface roughness of the granular [13–15]. Numerous investigators have attempted to measure the impact of particle diameter on the force of flow resistance. For example, the diameter of grains and porosity were shown by Carman et al. [16] as a function of the coefficient of the Kozeny–Carman equation. Another version of the well-known Ergun equation expresses the linear term and quadratic term coefficients as functions of particle diameter and porosity but uses the Kozeny–Carman expression for the linear term coefficient [17]. Several semi-empirical non-linear equations that considered the impact of particle size were proposed. These equations were derived from laboratory tests or analysis of existing data in the literature [18–23]. In this regard, it is also possible to define porosity as a function of particle diameter [16,21]. As a result, particle diameter makes sense as a key factor in flow field division.

For their experimental investigation into the pre-Darcy era, Siddiqui et al. [24] select an organic fluid and solidified petroleum rocks. They discover types B and C's pre-Darcy conduct. To prevent polar interactions that are common with aqueous fluids, an organic liquid and porous media combination is utilised. The researchers identified critical velocities below which their data exhibit a power-law behavior as opposed to a linear Darcy behaviour. A rising critical velocity was revealed with increased permeability in various porous materials. The researchers also explained the pre-Darcy behaviour as a result of a reaction between the consolidated porous media and the organic liquid. In the same context, Wang and Sheng [25] focused on the liquid threshold pressure gradient and the pre-Darcy flow phase. The flow regimes were separated by these researchers into two categories: (i) a linear flow regime (Darcy flow) for larger pressure gradients and (ii) a non-linear flow regime (non-Darcy flow) for smaller pressure gradients. Nevertheless, they concluded that the idea of a threshold pressure gradient is a misreading of the evidence from experiments. Specifically, no experimental data truly approaches a point of zero velocity; hence, any extrapolation in the lack of accurate data results in a pressure gradient that is not zero and has no physical significance.

To derive a novel relation for pressure drop in porous medium (rock fill), Sedghi-Asl and Rahimi [26] coupled the Darcy-Weisbach friction loss in open pipes with Manning's formula for open-channel flow. Manning's equation was confirmed with experimental data for the hydraulically rough regime. For Re <120, a linear Darcy regime; for Re between 120 and 10,000, a transitional regime; and for Re >10,000, a turbulent regime was shown to exist. The average particle diameter was used to calculate the Reynolds number.

Flow behaviour is necessary for flow field division. The "wall effect" [27–29] or the functional connection with linear term and quadratic term coefficients [30,31–33] were received the majority of attention in the link between flow behaviour and particle diameter up to this point. Several researchers were looked at the relationship between the ratio of bed-to-particle diameter and the porosity of packed beds [34,35].

Referring to the above discussed studies, the link between particle diameter and the flow transition criteria has not been thoroughly studied. It is clear that particle size variation affects flow transition significantly [36] and plays a crucial role in flow field division. Thus, a specific research on the connection between particle diameter and flow transition criterion—particularly turbulent onset—should be done.

The aim of the current research is to determine the impact of the particle size and the inlet velocity of water on the flow parameters through a porous media while solving the Brinkman equations for a more accurate simulation of the fluid flow. In the present investigation, it is intended to present an extensive understanding on the elevated pressure gradients, friction factors and Reynolds numbers by understanding their connection and how they affect flow characteristics in porous matrices. Finally, it is becoming clear that such discoveries would provide useful data for improving the overall effectiveness in designing and optimising engineering applications involving fluid transport processes through porous structures.

2. Methodology

In this research, a laminar, steady-state water flow through a porous media was modeled using the Computational Fluid Dynamics (CFD) and the effect of the particle size on velocity profile, pressure gradients distribution as well as friction factors were investigated. The numerical modelling employed here utilises the Brinkman-extended Darcy equations, which are appropriate for flow through porous media.

The particle size distribution of the porous medium was varied with different particle diameters that are more relevant to most engineering problems. Computational grid was then established using a structured mesh with higher density in zones where velocities and pressures are

gradients, especially in the inlet region and the porous media. In order to increase confidence in the accuracy of the numerical simulations, mesh optimisation and mesh independence analyses were performed.

The governing equations were solved using finite volume method while second order upwind discretisation applied to the spatial discretisation to improve solution accuracy. For the coupling of the pressure and velocity fields which is crucial in the SIMPLE algorithm, the convergence stability in the entire simulation was achieved. Boundary conditions were defined with a varying inlet velocity (from 0.001 m/s to 0.005 m/s) and a stationary pressure outlet. At the interfaces of the solid-fluid, the no-slip condition was used in order to model the interaction of the fluid with the porous matrix.

After the model was developed using the simulation results, the comparisons were made against experimental data and the Kozeny-Carman correlation in order to determine the quantitative accuracy of the model.

3. Numerical description

In this research, a numerical simulation according to the Brinkman-extended Darcy model was performed that is used to describe the flow of the fluid through the porous material. These equations consider both the viscous and the inertial terms of the fluid phase while interacting with the solid phase of the porous media. There are often a finite number of control volumes in the flow domain which are discretised using a structured mesh.

The governing equations were discretised using the finite volume method (FVM), which is also capable of preserving the mass, momentum and energy in the numerical formulation. Spatial discretisation was done using a second-order upwind scheme for both velocity and pressure fields. This scheme increases accuracy in the details of flow features especially at the vicinity of high gradients such as the inlet section and at the vicinity of the porous media.

For the pressure-velocity coupling, the SIMPLE algorithm therefore Semi-Implicit Method for Pressure-Linked Equations was employed. It is an iterative solver that is coupled and optimised to solve both continuity and momentum equations at one go and until they converge. Convergence was achieved using a convergence criterion of 10^{-6} for the residuals of the continuity, momentum and energy equations which yields a precise solution.

The boundary conditions were implemented as follows: at the inlet a steady flow velocity of between 0.001 m/s and 0.005 m/s was used while at the outlet pressure was set to 0-gauge pressure. The outer and internal surfaces of the porous medium were set with no-slip condition to represent the behaviour of the fluid and the solid phase effectively. The simulation was performed for different particle size to study its impact on flow parameter like velocity profiles, pressure gradient and friction factors.

The numerical simulations were performed using the ANSYS Fluent software, which provides robust solvers and pre-processing tools for meshing, setting boundary conditions, and running simulations. To ensure mesh independence, a mesh sensitivity analysis was conducted, with mesh refinement done in regions of high velocity and pressure gradients to improve solution accuracy.

4. Physical model and computational method

4.1. Governing equations

The fluid flows in the free channel and the porous medium block. The fluid flow enters at the lift side and leaves at the right side. The incompressible and stationary Navier-Stokes equations describe the free flow [37,38]:

- The equation of continuity (incompressible fluid)

$$\rho\left(\frac{\partial u_x}{\partial x}+\frac{\partial u_y}{\partial y}\right)=0 \tag{1}$$

- The equation of motion (momentum)

$$\rho\left(u_x\frac{\partial u_x}{\partial x}+u_y\frac{\partial u_x}{\partial y}\right)=-\frac{\partial P}{\partial x}+\frac{\partial}{\partial y}\left[\mu\left(\frac{\partial u_x}{\partial y}+\frac{\partial u_y}{\partial x}\right)\right] \tag{2}$$

$$\rho\left(u_x\frac{\partial u_y}{\partial x}+u_y\frac{\partial u_y}{\partial y}\right)=-\frac{\partial P}{\partial y}+\frac{\partial}{\partial x}\left[\mu\left(\frac{\partial u_y}{\partial x}+\frac{\partial u_x}{\partial y}\right)\right] \tag{3}$$

where u is the channel velocity (m/s), ρ is the fluid's density (kg/m^3), P is the pressure (Pa), and μ represents the dynamic viscosity (Pa·s). The flow in the porous domain is described by the Brinkman equations with Darcy law:

- The equation of motion (Brinkman equations)

$$\frac{\rho}{\epsilon_p}\left(u_x\frac{\partial}{\partial x}\left(\frac{u_x}{\epsilon_p}\right)+u_y\frac{\partial}{\partial y}\left(\frac{u_x}{\epsilon_p}\right)\right)=-\frac{\partial P}{\partial x}+\frac{\partial}{\partial y}\left[\frac{\mu}{\epsilon_p}\left(\frac{\partial u_x}{\partial y}+\frac{\partial u_y}{\partial x}\right)\right]-\frac{\mu}{\kappa}u_x \tag{4}$$

$$\frac{\rho}{\epsilon_p}\left(u_x\frac{\partial}{\partial x}\left(\frac{u_y}{\epsilon_p}\right)+u_y\frac{\partial}{\partial y}\left(\frac{u_y}{\epsilon_p}\right)\right)=-\frac{\partial P}{\partial y}+\frac{\partial}{\partial x}\left[\frac{\mu}{\epsilon_p}\left(\frac{\partial u_y}{\partial x}+\frac{\partial u_x}{\partial y}\right)\right]-\frac{\mu}{\kappa}u_y \tag{5}$$

κ denotes the permeability of the porous medium (m^2), ε_p is the porosity (dimensionless).

To minimise the discrepancy that may arise from approximations in the derivation of the momentum equations, the diffusive term has been corrected to reflect the Laplacian of the velocity as indicated in Eqs. (4) and 5. Also, the effective viscosity of the fluid was accepted to be μ/porosity from the perspective of mathematical modelling in porous media.

It is also pointed out that the permeability K in the Darcy term was considered a scalar, which is appropriate for isotropic porous media. However, in anisotropic media, permeability is normally depicted in form of a second order tensor to give account of the directional variation in flow resistance. This simplification is in consistent with the isotropic conditions presumed in the current study.

4.2. Fluid-porous medium boundary

The above model has been extended by adding the right boundary conditions, especially those on the interface of the fluid and the porous structure. The boundary conditions assumed are as follows:

1) No-slip condition at the solid-fluid interface: Nonetheless, for the primary set of conditions it is customary to set no slip in the fluid at the interface with the porous matrix, that is, $v = 0$ at the boundary of the porous medium.
2) Continuity of normal stress: It is assumed that the pressure at the fluid-porous interface is well defined so that there is no discontinuity in pressure across the interface.
3) Permeability model: The porosity of the medium is also taken to be isotropic in the present investigation and the Darcy term is taken to be scalar. The same could be said for more complex media; the permeability could be described as a tensor as was also noted in the textual material above.

4.3. System parameters and fluid properties

In order to eliminate the inlet effect, the inlet and outlet sections are extended. Table 1 shows the main property parameters used for simulation. Also, Table 2 presents the properties of water used for simulation.

Fig. 1 depicts the two-dimensional geometry of the system employed in computational fluid dynamics (CFD) analysis of Darcian flow through porous media. Geometry is created as a simplified physical model in which fluid is introduced from the left side of the computational domain and removed from the right side in order to study the flow behaviour inside the defined porous media. The free flow channel alongside a porous block is a part of the configuration that is paramount in the study of the fluid and porous structure interrelation. Such a configuration allows for proper utilisation of the Navier-Stokes equations that apply to the free flow zone and the Brinkman equations that apply to the porous zone; such a feature allows for a complete analysis of pressure and velocity fields in the system. The 2D representation helps to define the flow paths and boundary conditions, which are crucial for correct modelling of the dynamic of fluid movement as upon changes of various parameters, including the inlet velocity, and the grain size of the porous material.

In this research, the analysis was conducted in two-dimensional format because of the demanding computational loads involved, although this approach preserved the core mechanics of the flow within the porous matrix. This approach enables a more effective probing of the behaviour of the fluid under the specified conditions whilst at the same time not producing a large number of results for the purpose of the study as planned. Although the geometry of the medium is cylindrical, the Cartesian coordinate system was selected because of its compatibility with a mathematical numerical solution and because it provides sufficiently accurate characteristics of the flow in a simplified region.

The assumptions of the model are strictly valid at steady-state conditions, incompressible and Newtonian fluid, isothermal flow, no-slip condition at the solid-fluid interface and negligible inertia effects when the flow is described by Darcy's law and when the flow is in the Brinkman domain. These assumptions help to factor out or eliminate other aspects which would otherwise complicate the study of the flow characteristics through porous media in relation to particle size and inlet velocity. Admittedly, it is possible to use a cylindrical coordinate system or the vectorial form of the considered equations that would provide a better approximation of the real geometry and flows. Their inclusion in future investigations would facilitate a better understanding of the flow dynamics during circumstances when 3D effects and complicating geometries have a drastic impact.

4.4. Meshing

Meshing scheme and discretisation of computational domain used in the Brinkman model to simulate fluid flow through porous media is shown in Fig. 2. Meshing is an important tool in CFD since it involves conversion of a continuous domain into discrete elements for numerical analysis of governing equations [40]. In areas of velocity /pressure gradients the figure shows a greater mesh refinement around the external boundaries of the pore structure and through the channel. This refinement is aimed at improving the precision of the simulation by guaranteeing that solutions given numerically give a clear image of the flow patterns and the flux throughout the combination of the fluid and porous media. The availability of triangular and quadrilateral elements in the mesh type proves suitable for the description of the flow geometry. The minimum and average element quality are shown and these values characterise the quality of the mesh as a whole as well as being crucial for convergence in simulations of Darcian flow dynamics.

Table 3 shows the mesh statistics that were adopted for the CFD modelling of Darcian flow in porous media to give information on the quality and the constituents of the mesh used in the simulation. It comprises measures like the minimum and average element quality which provide information concerning the compliance of the mesh to the domain geometry, and the applicability of the elements for analysis. This is further supported by a global minimum of 0.2294 and an average of 0.8137 which shows that despite there being some sub-optimal elements the mesh is fine for simulated purposes. The table also summarizes the detail mesh into various kinds of elements such as 74,774 triangular parts and 7914 quadrilateral parts and 2772 edge of elements.

Table 2
Water properties used for simulation.

Property	Value	Unit
Density (ρ)	998.20	kg/m^3
Viscosity (μ)	0.00101	Pa s

4.5. Model validation

Fig. 3 shows the comparison of simulation results for each particle size with the experimental results of Li et al. [39] and the correlation proposed by Kozeny and Carman [41,42]. The formula proposed by Kozeny and Carman is expressed as Eq. (6). The figure also shows that the simulation results are more consistent with the Kozeny and Carman correlation with an error per cent of 4 % than the experimental results of Li et al. [39] with an error per cent of 10 %, which are acceptable percentages for industrial design. This confirms the validity of the model.

$$\frac{\Delta P}{L} = 180\,\frac{\mu\, u_{pm}}{d_p^2}\,\frac{\left(1-\epsilon_p\right)^2}{\epsilon_p^3} \tag{6}$$

A few things worth remembering are that the Darcy's law with the Brinkman correction is only applicable to the creeping flow regime where inertial effects are negligible. In the higher flow regime where inertia is present, the permeability is determined by the shape of the porous material as well as inertial factors. This limitation might be the reason why deviations from the Kozeny-Carman equation are observed in the experimental data shown in Fig. 3.

The Kozeny-Carman equation prescribes purely geometrical factors

Table 1
Main property parameters used for simulation [39].

Property parameter	Value					Unit
Cylindrical container diameter (D)	100					mm
Cylindrical container length (L)	500					mm
Inlet length	500					mm
Outlet length	500					mm
Inlet velocities range (u)	0.0034 – 0.017					m/s
Inlet velocities range of porous medium (u_{pm})	0.001 – 0.005					m/s
Material of particles	Granular silica sands					–
Diameter of particles (d_p)	1.075	1.475	1.85	2.5	3.17	mm
Aspect ratio (D/d_p)	93.023	67.797	54.054	40	31.546	–
Porosity (ϵ_p)	0.39914	0.39915	0.39914	0.39915	0.39915	–
Permeability (κ)	1.0453×10^{-9}	1.6453×10^{-9}	2.1901×10^{-9}	2.4207×10^{-9}	2.8752×10^{-9}	m^2

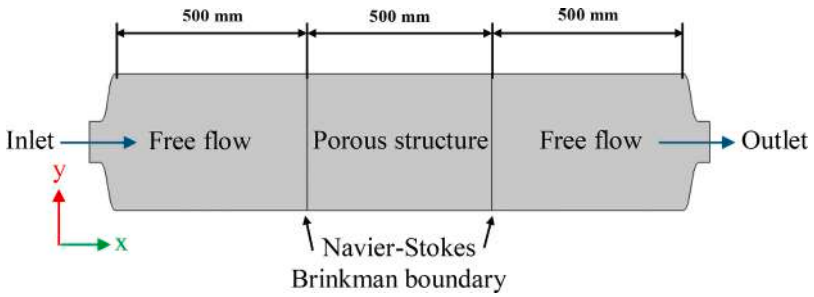

Fig. 1. Depiction of the 2D system geometry.

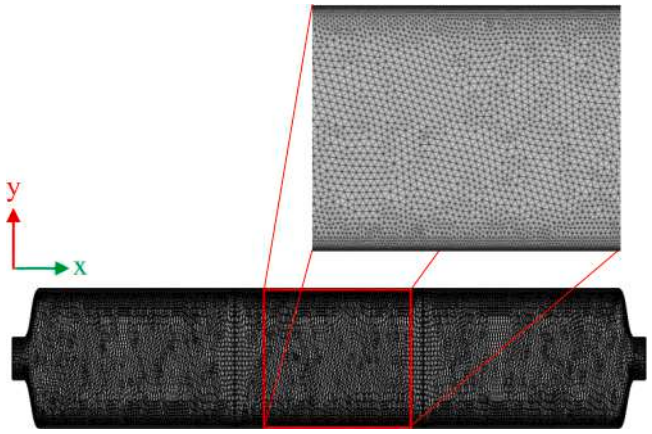

Fig. 2. Typical meshing scheme and discretisation of the domain of finer size in the Brinkman model.

Table 3
Mesh statistics.

Element quality	Coarse	Normal	Fine
Number of elements	12,050	18,790	34,300
Minimum element quality	0.2298	0.2110	0.2478
Average element quality	0.7653	0.7840	0.7740
Triangle	9938	16,078	30,898
Quadrilateral	2112	2712	3402
Edge element	781	1003	1258
Computation time	12 s	*16 s*	18 s

controlling permeability, and thus, is invalid at higher flow velocities. Thus, differences in the data suggest that non-linear corrections or other models should be used for the description of flow characteristics in the given conditions.

4.6. Data processing

The calculation formulas for the Reynolds number, friction factor, and pressure gradient are as follows [43,44]:

$$Re = \frac{\rho d_p u_{pm}}{\mu} \tag{7}$$

$$f = \frac{\Delta P}{L}\frac{d_p}{\rho u_{pm}^2}\frac{\epsilon_p^3}{(1-\epsilon_p)^2} \tag{8}$$

$$\frac{\Delta P}{L} = f\frac{\rho u_{pm}^2}{d_p}\frac{(1-\epsilon_p)^2}{\epsilon_p^3} \tag{9}$$

$$\frac{\Delta P}{L} = \frac{\mu}{\kappa}u_{pm} \tag{10}$$

4.7. Boundary conditions

All the simulations were performed by taking water as an incompressible fluid with inlet velocities of 0.0034 m/s, 0.0068 m/s, 0.0102 m/s, 0.0136 m/s, and 0.016 m/s, respectively. The boundary conditions for the model equations are outlined below:

- At $x = x_{in}$ and $x = x_{out}$

$$\frac{\partial u_x}{\partial y} = u_y = 0 \tag{11}$$

- At the inlet of porous medium $x = 0$

$$u_x = u_{pm} = 0.001\frac{m}{s},\ 0.002\frac{m}{s}, 0.003\frac{m}{s}, 0.004\frac{m}{s},\ 0.005\frac{m}{s} \tag{12}$$

- At the outlet of porous medium $x = 500$

$$P = P_0 \tag{13}$$

The velocity boundary condition in Eq. (12) describes the inlet of the porous medium by following the conventional methods that are utilised in the modelling of porous media. Velocity and stress boundary conditions are applied within the fluid-porous medium interface. In particular, the no-slip condition is imposed on the solid-fluid interface; that is, the velocity vector is assumed to be zero at the interface. This approach maintains conformity to prior methods used in modelling of the fluid flow in the porous media.

5. Results and discussion

5.1. Velocity contour of porous media

Figures below-described velocity contour map depicted in Fig. 4 illustrates the fluid velocity profile in the porous medium of particle size 3.170 mm under CFD analysis. The contour plot implies the strength of the fluid velocity at different point within the domain to help understand how the fluid flows through the porous media. The narrow contour intervals imply high velocity gradients, and are represented, where the lines are closely placed, suggesting that velocity tends to change rapidly in that region. Conversely, larger distances between these contour layers indicate regions with relatively small velocity gradients, signifying regions in which the fluid is less turbulent and at a more consistent speed. This map could be useful in elucidating the relationship between the fluid and the solid phase of the porous media. It assists in determining the regions where the fluid accelerates or decelerates while in the medium and the roles played by particle size and permeability of the porous material. For example, near the inlet, the velocity of the fluid is normally high, especially because the flow enters under pressure and is more

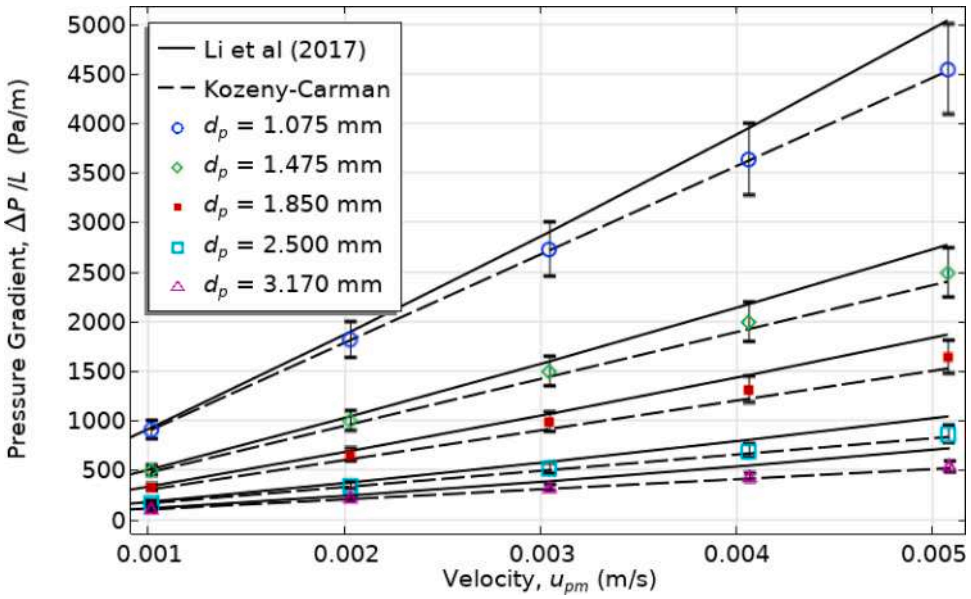

Fig. 3. Validation of pressure gradient at various inlet velocities for each particle size.

active. As the fluid penetrates further into the porous body its velocity decreases by virtue of the solid particles that offer resistance and as result there are areas with notably low velocity. Moreover, the contour map can show the existence of areas with low velocity or recirculating zones, which are important for characterising the flow patterns inside the porous media. Dead water zones are areas where there is little or no fluid movement, they occur in low permeable zones or where movement of the fluid is restricted by particles. Recirculation regions, in contrast, refer to those areas in which the fluid actually flows in the reverse direction; that is, there are stagnation zones. These phenomena are of special concern when evaluating the effectiveness of the fluid transportation within the porous matrix. In the field of filtration, groundwater recharges, or catalytic reactors, these areas may have major impacts on the performance of the system since they may either improve or deteriorate the flow and mixing of fluids, the mass transfer or the efficiency of particle trapping or pollutant dilution.

Thus, analysis of these velocity profiles provides engineers with important information about the efficiency enhancement for the design of porous media systems as well as overall improvement of the function of systems using porous materials.

5.2. Axial-Averaged velocity in porous media

Fig. 5, the velocity profile showing inlet velocities of the fluid flow through the porous medium comparing the effect of flow rate on the velocity distribution in the system. The profiles are developed at a particular cross-section of the porous medium and these demonstrate how different inlet velocities affect flow in the system. We also notice that as the inlet velocity increases, or the velocity profile transforms where the peak is more centrally located near the inlet and the velocity gradient reduces as it moves deeper into the region of porous media. These findings suggest that at high flow rates the inertial contribution has higher value, because the shear forces acting upon the fluid increases. The figure also shows the influence of different parameters characterising the porous medium like particle size and porosity on the velocity distribution as these factors change the degree of resistance offered to the flow of the fluid through the permeable medium. These profiles show that for low velocities of inlet flow, the activities have a higher possibility of being laminar and homogenous while at higher velocities possess some form of turbulence.

5.3. Pressure contour of porous media

Pressure distribution map is represented in Fig. 6 showing pressure variations in the flow domain of the porous media under the given flow conditions exerted from the CFD simulation analysis. The lines reflect the distribution of the pressure across the domain while dense lines depict high pressure area while the lines are wide show the low-pressure area. Fig. 6 shows that pressure usually declines going from the inlet to outlet and this is because, just like in any other system most fluids lose some of their energy by way of friction and resistance whenever they pass through a porous medium. Further, the boundaries may encourage visualisation of regions of pressure drop, which may arise from alterations in the geometry of the porous media, or variability in particle size, which may give rise to stagnation or recirculation zones in the flow path.

5.4. Pressure in porous media

Local pressure distribution is shown in Fig. 7 with the help of which pressure variation in the porous medium at specific points by changing the inlet velocities of the flow can be understood. On the graph or contour map, usually the pressure, distance or specified zones of the porous structure is compared with the pressure gradient or variation of pressure with any particular inlet velocity. The figure also reveals that as the inlet velocity increases, the quantified local pressure reduces, more precisely nearly at the inlet zone where the fluid flow is full of kinetic energy and encroaches into the porous media. This reduction in pressure reflects the higher flow rate velocity and the consequential losses due to the interfacial friction between the fluid and the porous structure.

5.5. Comparison of particle size effects

The velocity contour plot at an inlet velocity of 0- 0.001 m/s for the flow through a porous medium is shown in Fig. 8, which represents the distribution of fluid velocity throughout the domain in terms of contour plot at this particular flow rate. The changes in the velocity of the solar wind are portrayed by the proximity of the lines to one another; the closer, the higher velocity and the lines farther apart show lower velocity. At this low inlet velocity, the flow is laminar, which means it has an orderly flow of the fluid elements. The contour map shows that high velocities are achieved in the vicinity of the inlet where the fluid first invades the porous media and reduces as the fluid continues to infiltrate

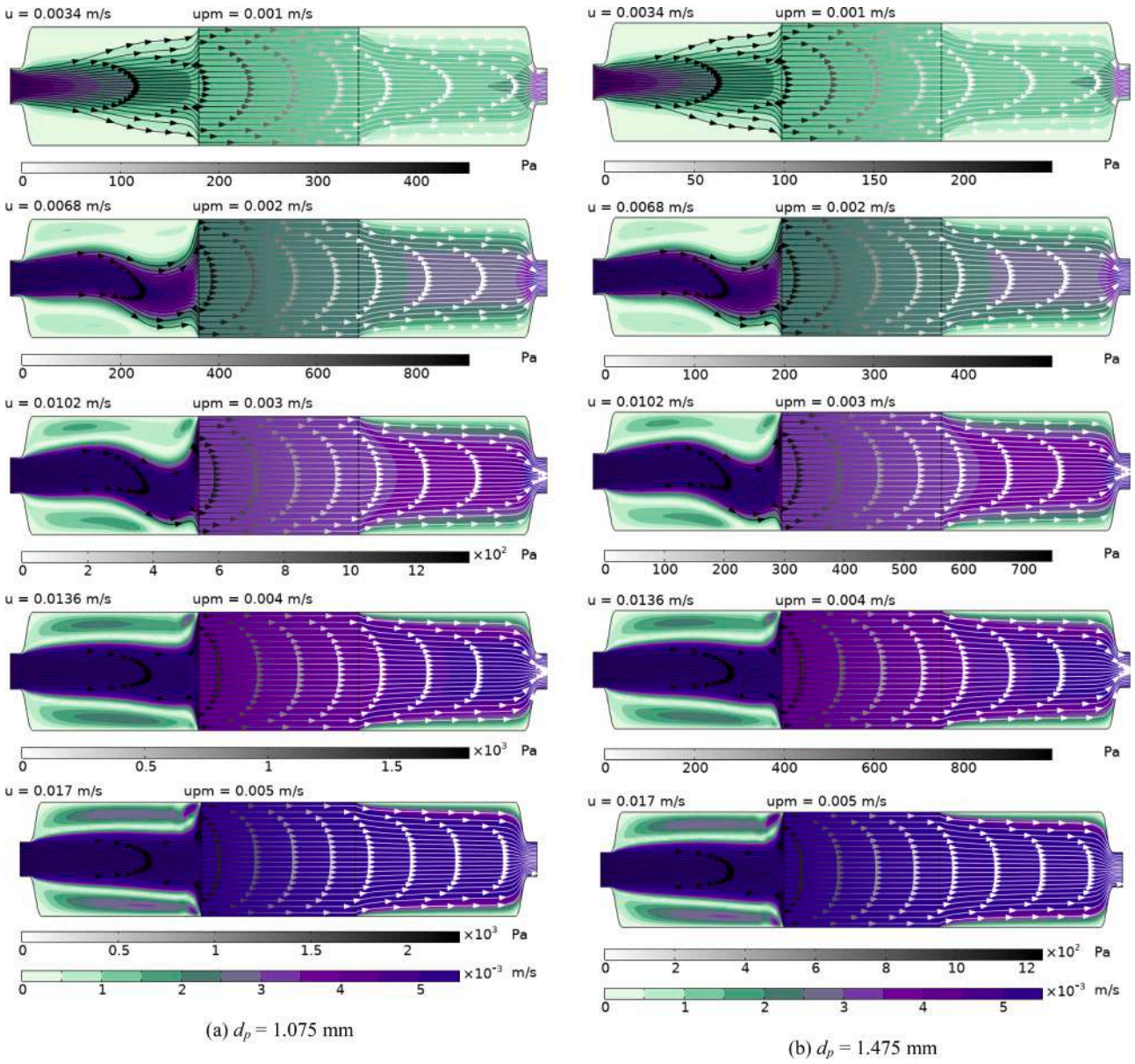

Fig. 4. Velocity contour.

into the pores of the media. This behaviour is noted due to action of the matrix which offers stiff resistance to the flow of the fluid especially as it moves within the interstitial space between particle.

The variation of velocity for fluid flow through the porous medium at inlet velocity of 0.001 m/s in a particular cross-section of the medium is shown in Fig. 9 known as velocity profile. The profile normally involves a plot of velocity against distance from the inlet and takes a certain shape owing to laminar flow at this velocity. The velocity is highest at a point near the inlet due to its direct interaction with the inlet conditions and as the fluid continues to progress within the porous matrix, the velocity begins to reduce further. This decrease is mainly due to the shear stress that the fluid experiences as it comes into contact with the solid particles within the porous material. The profile might be parabolic or linear which also shows a smooth change in velocity, and this is common with the laminar flow where the forces of viscosity are dominant.

Fig. 10 depicts that pressure contour map of the fluid flow through the porous media for inlet velocity 0.001 m/s has been drawn to analyse pressure distribution in the porous media under such flow conditions. This map portrays various degrees of pressure where the thick lines denote areas of high pressure and extended lines are areas of low pressure. At this low inlet velocity, the pressure drop is normally large on entry into the porous media where they meet resistance from the solid phase. Taking a look at the contour map below, it shows that pressure increases along the inlet up to the point of injection and then decreases as the fluid go deeper into the reservoir. This pressure drops manifests through frictional losses and fluid and structure interactions in a porous medium.

Fig. 11 shows a clearly explained picture of local pressure changes in the flow porous medium at the inlet velocity of 0.001 m/s, In Fig. 11, it is possible to understand how the pressure is distributed in particular areas of the flow field. This figure is generally in form of graph or data points that describe pressure distribution for a given pressure at several crosses marked with distances from the inlet. At inlet, the pressure has its maximum value because is directly exposed to the influence of the incoming fluid, but the it departs from this level as the fluid invades more deeply the porous structure and decreases in a considerable form. This is mainly due to the irreversible energy dissipation when the fluid

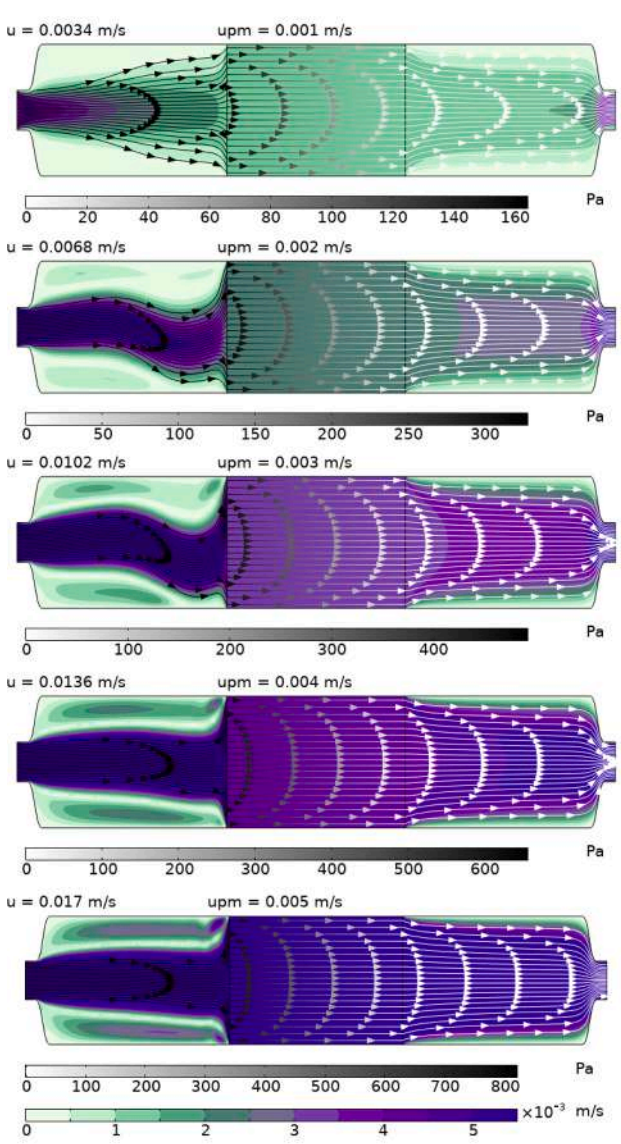

(c) $d_p = 1.850$ mm

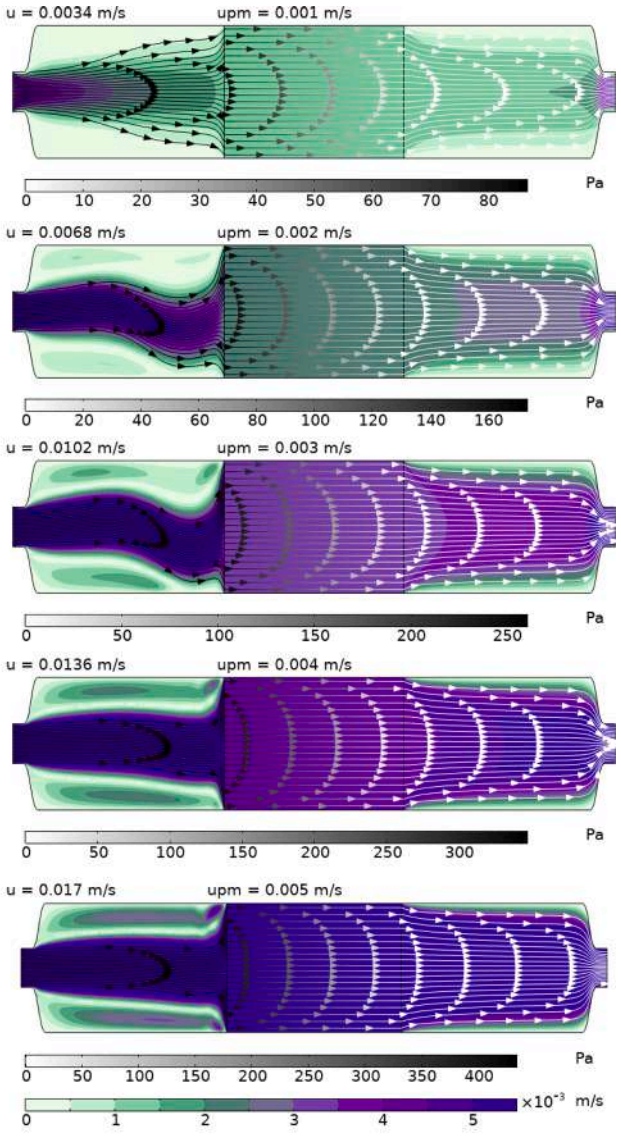

(d) $d_p = 2.500$ mm

Fig. 4. (*continued*).

seeks to flow through the matrix resistance offered by the porous material.

Fig. 12 exhibits the distribution of friction factors against inlet velocities for the various particle sizes in the porous medium to reveal the findings of the experimental examination of the relationship of these parameters. The figure commonly displays a graph of the friction factor to the inlet velocity for each particle size showing different trends/ relations. Because of effects of the Reynolds number it can be observed that as the inlet velocity increases the friction factor may decrease due to transition from laminar to turbulent, but the behavior can be different because of the grain size. Generally, the smaller the particles, the greater the interaction surface and therefore a greater ability to generate friction and potentially higher friction factors at lower velocities and larger ones while providing smoother flow paths and lower friction factors.

The friction factors that have been calculated in this study and the relationships developed conceals the effects of particle sizes within the porous phase of the medium on the Reynolds numbers and flow resistance derived in Fig. 13. In this figure, the friction factor is obtained based on Reynolds number for different particle sizes to observe the flow characteristic modification with the altering flow conditions. Normally, when the Reynolds number is increased to point where the flow pattern changes from laminar to turbulent, the friction factor might decrease mainly because of the improved mixing and diminished relative effect of viscous forces. However, it is not expected that the relationship is linear across all sizes of the particle; the particles sizes that are smaller are likely to produce higher friction factors at lower Reynolds numbers because of the increased surface area and resistance, while the larger particles may produce lower friction factors under turbulent flow.

Fig. 14 shows the features of the pressure gradient dependence on inlet velocities and the particle size in the porous media. In this figure, the pressure gradient is conventionally graphed against the velocity of inflow for the different particle sizes and the resulting curves distinguishable trends of interaction between flow velocity and particle characteristics. In the same manner, as the inlet velocity increases, the pressure gradient normally follows this trend showing that with increased rates of flow within the inlet duct result in added pressure losses due to friction and, or/interaction with the porous media. Although, with regards to the rate of increase in the pressure gradient several considerations should be made; Small particles reduce the passage cross sectional area hence increasing resistance thus steep pressure

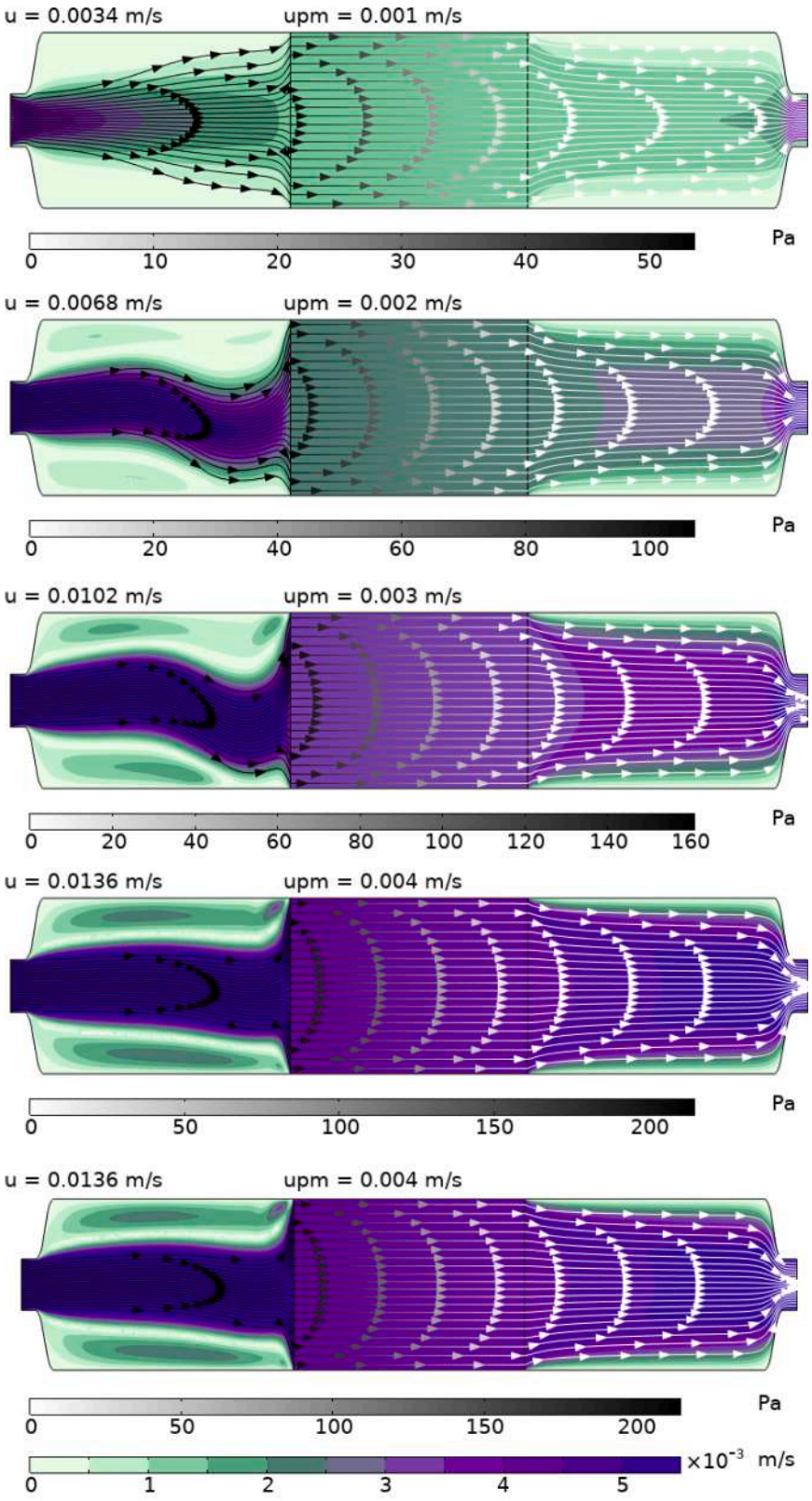

(e) $d_p = 3.170$ mm

Fig. 4. (*continued*).

gradients achieve at low velocity while large particles provide smooth paths hence more gradual pressure gradients.

Fig. 15 elaborates the characteristics of pressure gradient p have been plotted against Reynolds numbers for various particle sizes in the porous medium. On this figure one can infers how the pressure gradient vary with the Reynolds number or how the flow regime, whether Lamina

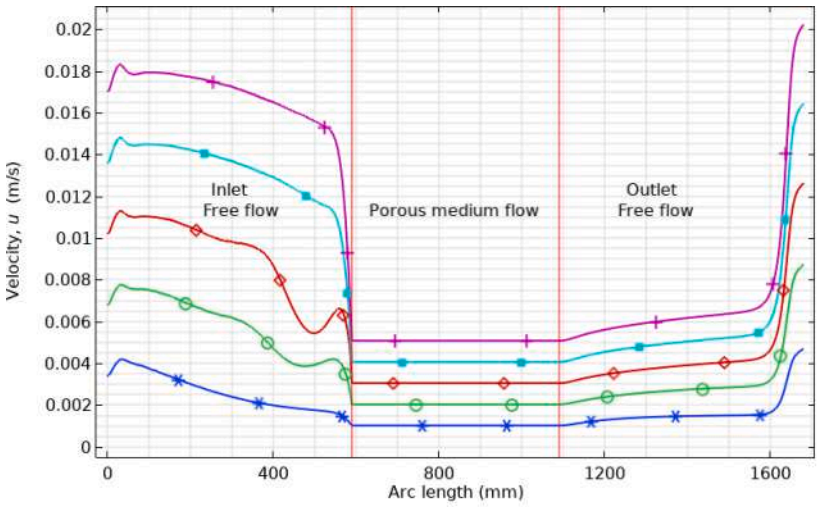

(a) $d_p = 1.075$ mm

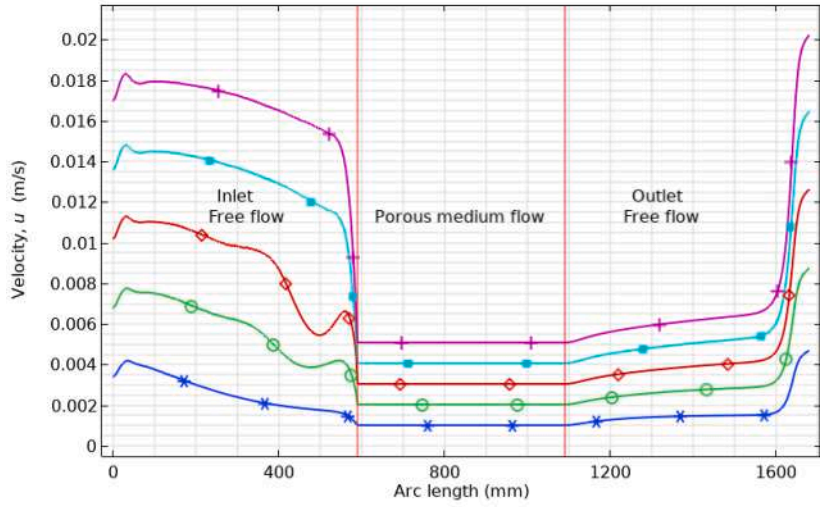

(b) $d_p = 1.475$ mm

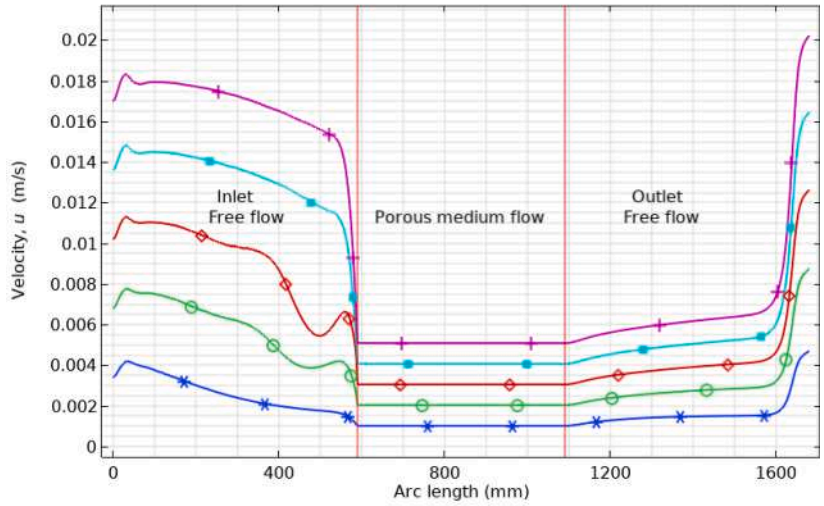

(c) $d_p = 1.850$ mm

Fig. 5. Velocity profile under different inlet velocities.

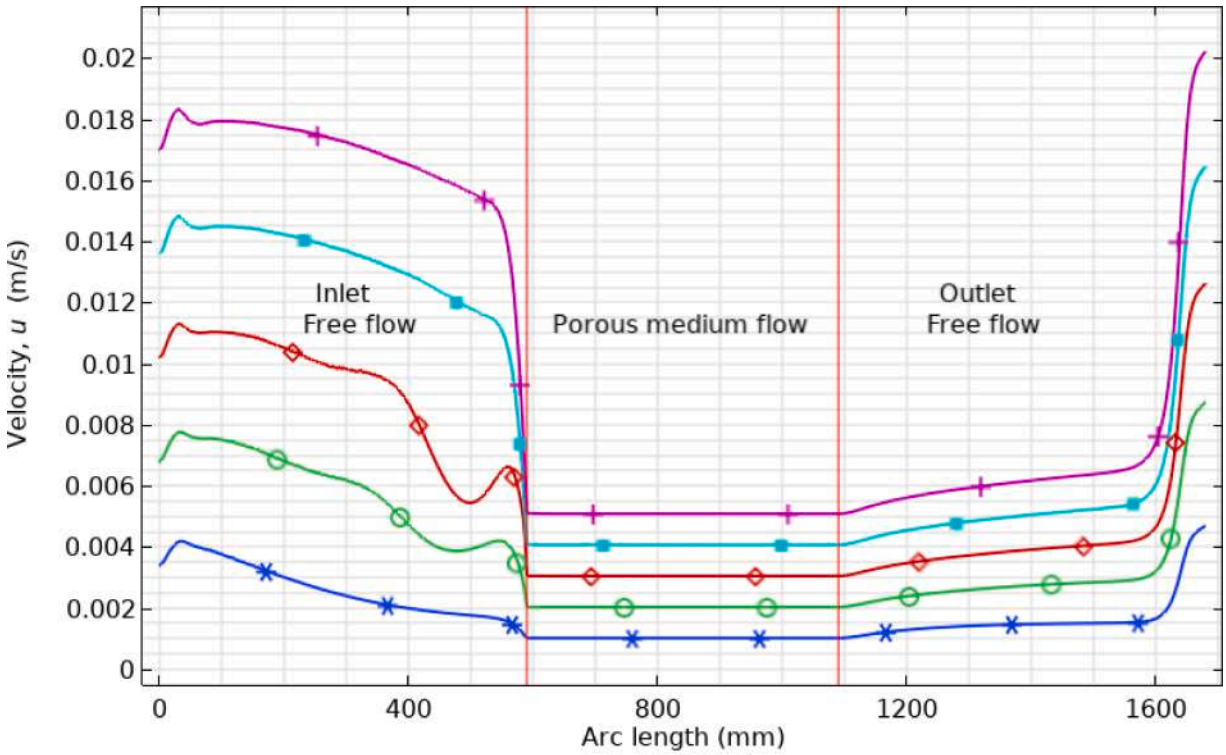

(d) $d_p = 2.500$ mm

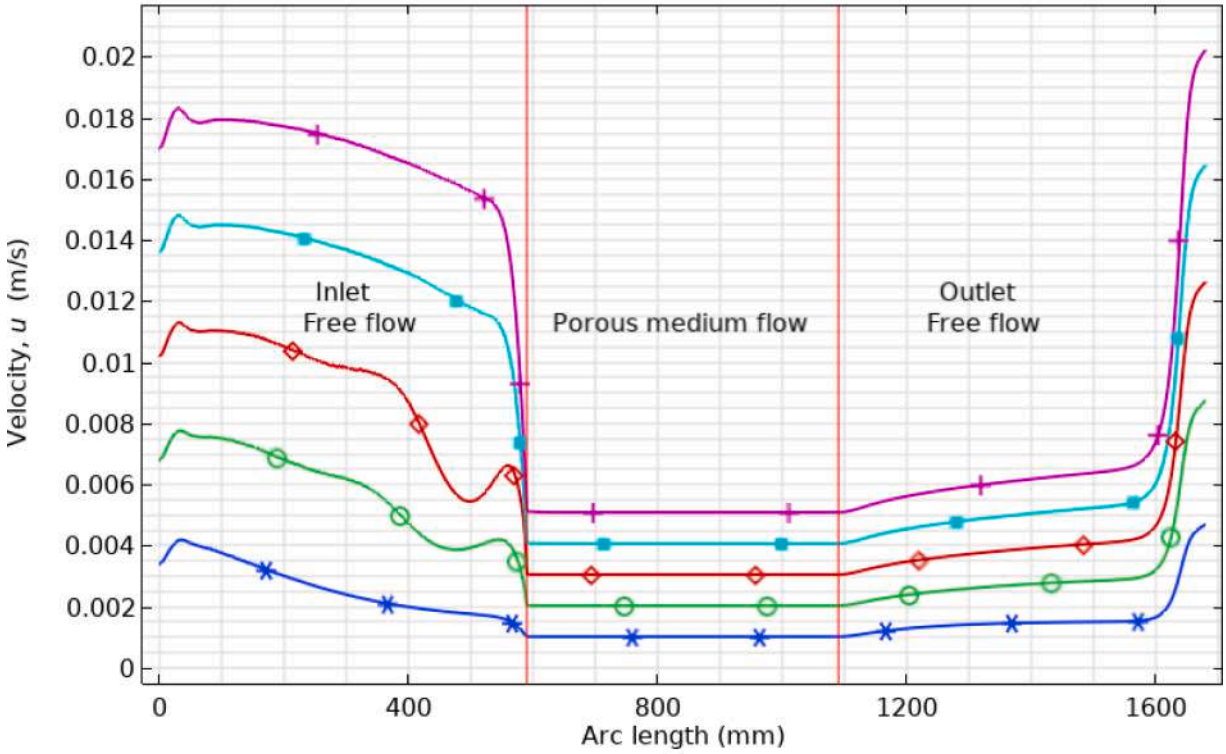

(e) $d_p = 3.170$ mm

Fig. 5. (*continued*).

or Turbulent, influence the pressure loss of the fluid for different particle size. With an increase in the Reynolds number signifying a transition to turbulent flow, the pressure gradient trend is generally steeply upwards as a result of increased shear stresses and turbulent interference with the flow. However, for pressure gradient, the increase in Reynolds number of the flow may not produce similar response for all particle sizes; weight small particles tend to increases pressure gradient at lower Reynolds numbers due to the high surface area and the high resistance of

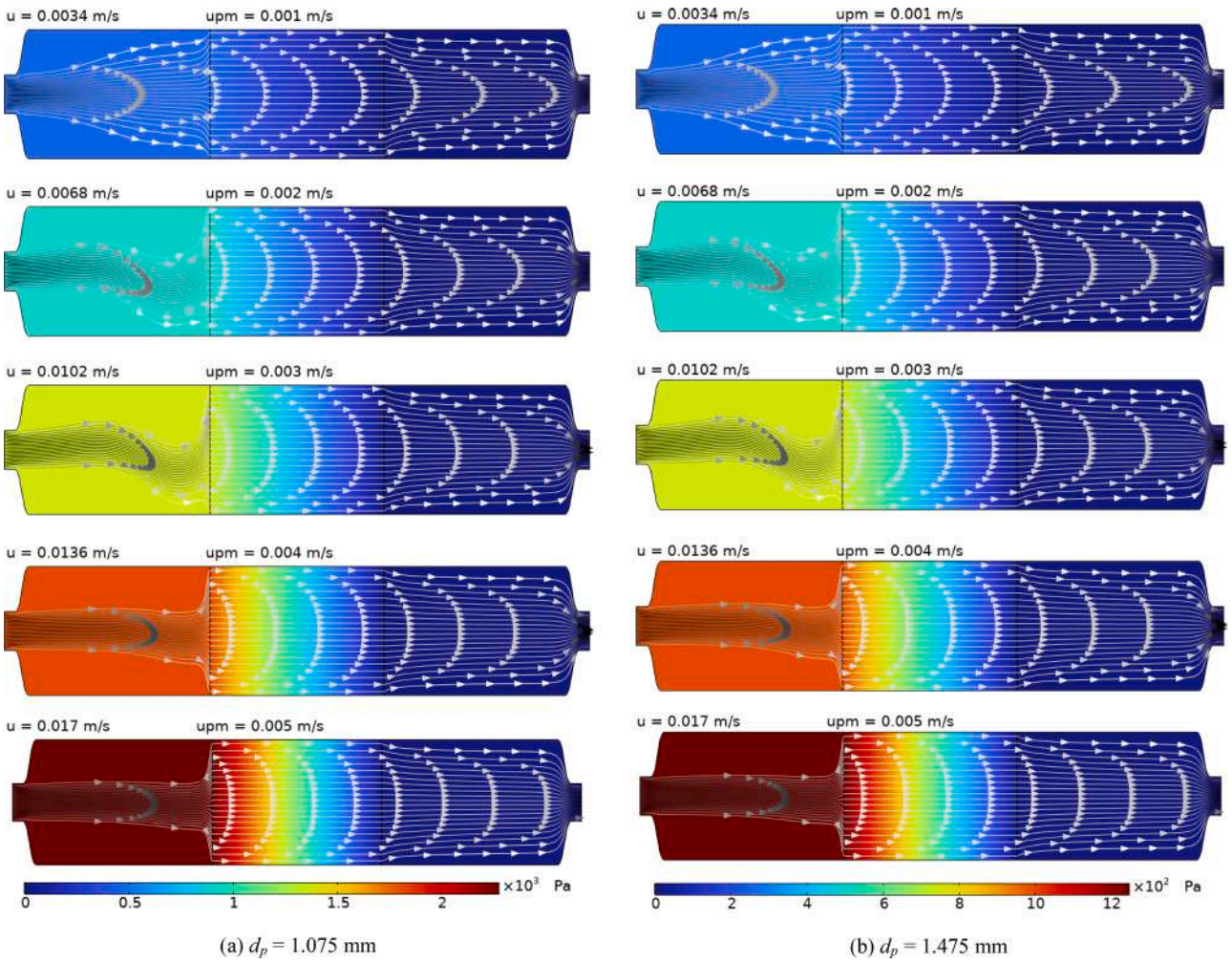

Fig. 6. Pressure contour.

the particles, on the other hand, weight larger particles may cause lower pressure gradient at higher Reynolds number as turbulence of the flow overwhelms the viscous effects.

6. Conclusions

In the current research, an investigation of the steady water flow through a porous medium was accomplished while applying the Brinkman equations for the imbibition dynamics affected by particle diameter and inlet velocity. Thus, the obtained results are essential for the description of fluid flow through porous structures, which is of great importance for many applications in engineering, such as filtration, groundwater management, and soil drainage. The following key conclusions can be drawn from the study:

1) The data of the current research showed that when the particle size is small, the friction factors and the pressure gradients at low velocity are higher if compared to large particles.
2) The results ascertained that an increase of inlet velocity would increase the pressure gradient and friction factor. This goes to show that higher flow rates translate to better opposed flow and energy losses inside the porous structure.
3) It has been clarified that the Reynolds number is a vital factor in signifying the flow regime. The quadratic dependence of pressure gradients with Reynolds numbers is verified as the flow evolves from laminar to turbulent, which can be useful in controlling flow rate of fluids through porous materials.
4) The pressure gradient, friction factor, inlet velocity and Reynolds number were all found to have a non-linear relationship.
5) The current analysis elaborated that pressure gradient behavior is greatly sensitive to the particle size and the flow rate. Referring to this notion, these parameters must be considered when designing and modelling fluid systems in porous media.
6) The friction factors have a high dependency on Reynolds number and particle size.
7) The current research presented the range of flow parameters at which flow properties should to be monitored to attain effective application of techniques dealing with particle laden flows.
8) The obtained information above is vital for enhancing designs and characteristics of systems containing porous media. It provides advice on how to decrease energy losses and improve transport of fluids in industrial uses such as separation, production of oil, and aquifers.
9) Employment of other techniques such as 3D simulations and multi-scale modelling can be considered to overwhelmed the drawbacks of 2D models and get better understanding of real-world problems.

7. Recommendations for future work

For future studies, it is recommended to focus on the following areas to further enhance the understanding of fluid dynamics in porous media:

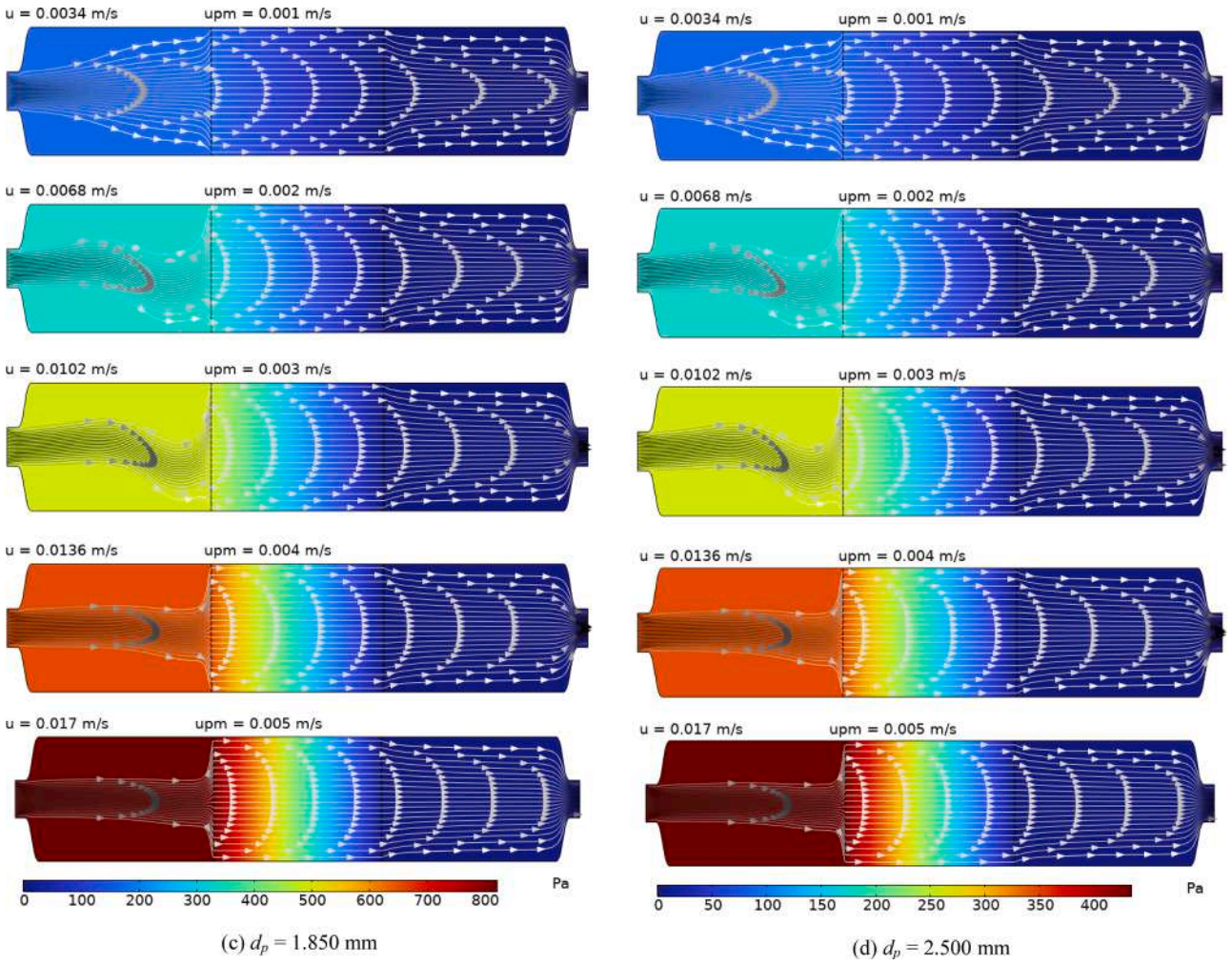

Fig. 6. (*continued*).

1. Investigating the effects of variable fluid properties, such as viscosity and density, on the flow behaviour in porous media would provide deeper visions into the relationship between these properties and flow resistance. Experimental studies with different fluids, including non-Newtonian fluids, could offer valuable comparisons with the current findings.
2. Future research could discover the effect of different porous media geometries (e.g., irregular, fractured, or hierarchical pore structures) on flow dynamics. Advanced imaging techniques such as X-ray tomography or 3D printing could be used to produce more realistic porous structures for simulations.
3. While the current research emphases on steady-state flow, inspecting transient flow behaviour, such as pressure fluctuations and flow rate variations over time, can afford a more complete understanding of the fluid dynamics in practical implications.
4. Simulating multi-phase flow in porous media could be a significant extension of the current research. These simulations would represent real-world systems, such as petroleum reservoirs or environmental contamination scenarios.
5. As the flow transitions from laminar to turbulent, refining turbulence models to precisely forecast the transition could be useful for capturing the impacts of high Reynolds numbers on flow behaviour in porous media, particularly for applications like filtration and soil drainage.
6. Exploring the scalability of the current model to larger systems, such as industrial filtration or groundwater management, could be a valuable direction for future research. This would involve validating the findings at a larger scale and developing optimisation strategies for industrial applications.
7. Further work may endeavour to replicate the results through experimental evidence to increase the practical application of the numerical simulations and the link to physically realised systems.

The above demonstrated areas would contribute to a more comprehensive understanding of fluid flow in porous media and help in optimising the design and performance of systems that rely on such processes.

CRediT authorship contribution statement

Asseel M.Rasheed Al-Gaheeshi: Writing – review & editing, Writing – original draft, Visualization, Validation, Supervision, Software, Project administration, Methodology, Investigation, Funding acquisition, Formal analysis, Data curation, Conceptualization. **Farhan Lafta Rashid:** Writing – review & editing, Writing – original draft, Visualization, Validation, Supervision, Software, Resources, Project administration, Methodology, Investigation, Funding acquisition, Formal analysis, Data curation, Conceptualization. **Mudhar A. Al-Obaidi:** Writing – review & editing, Writing – original draft, Visualization, Validation, Supervision, Software, Resources, Project administration, Methodology, Investigation, Formal analysis, Data curation. **Karrar A. Hammoodi:** Writing – review & editing, Writing – original draft, Visualization, Validation, Software, Resources, Methodology, Investigation, Formal analysis. **Ephraim Bonah Agyekum:** Writing –

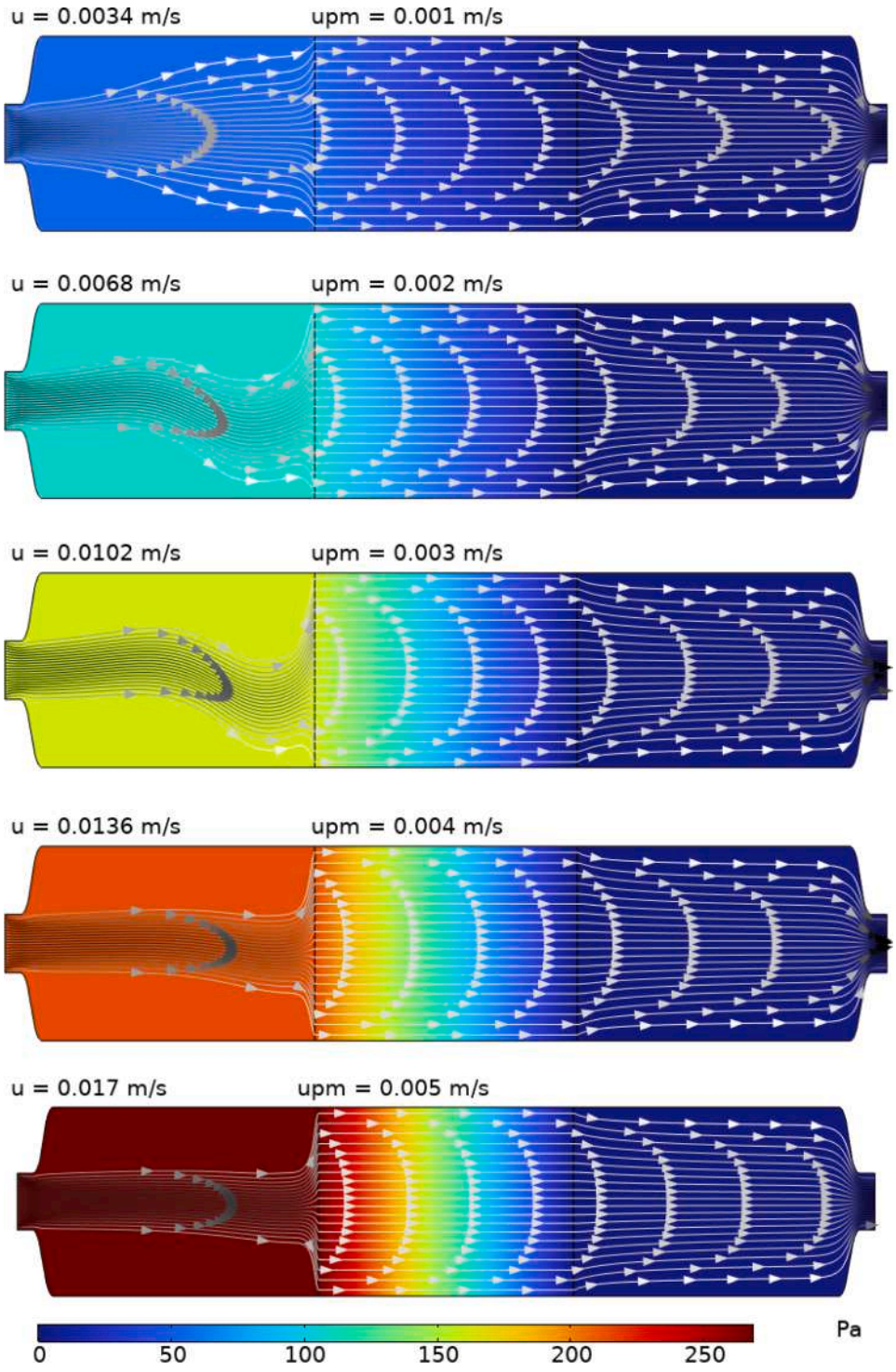

(e) $d_p = 3.170$ mm.

Fig. 6. (*continued*).

review & editing, Writing – original draft, Visualization, Validation, Supervision, Software, Methodology, Funding acquisition.

Declaration of competing interest

The authors declare that they have no known competing financial interests or personal relationships that could have appeared to influence the work reported in this paper.

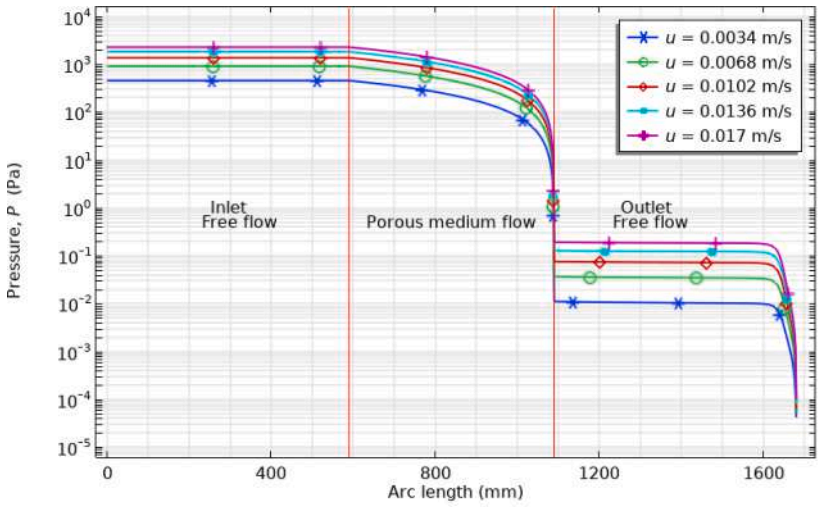

(a) d_p = 1.075 mm

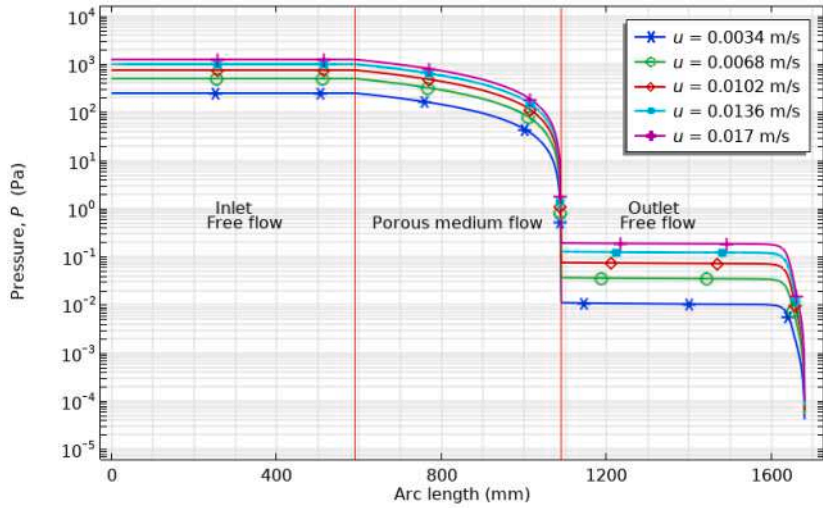

(b) d_p = 1.475 mm

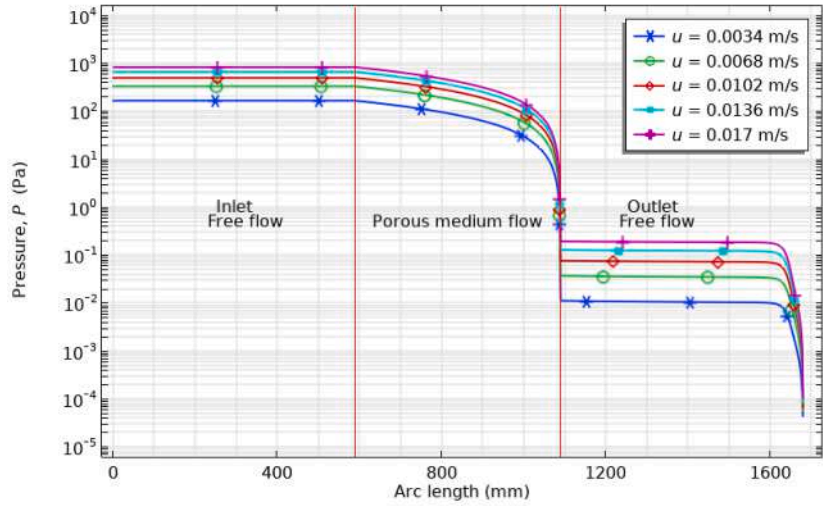

(c) d_p = 1.850 mm

Fig. 7. Local pressure under different inlet velocities.

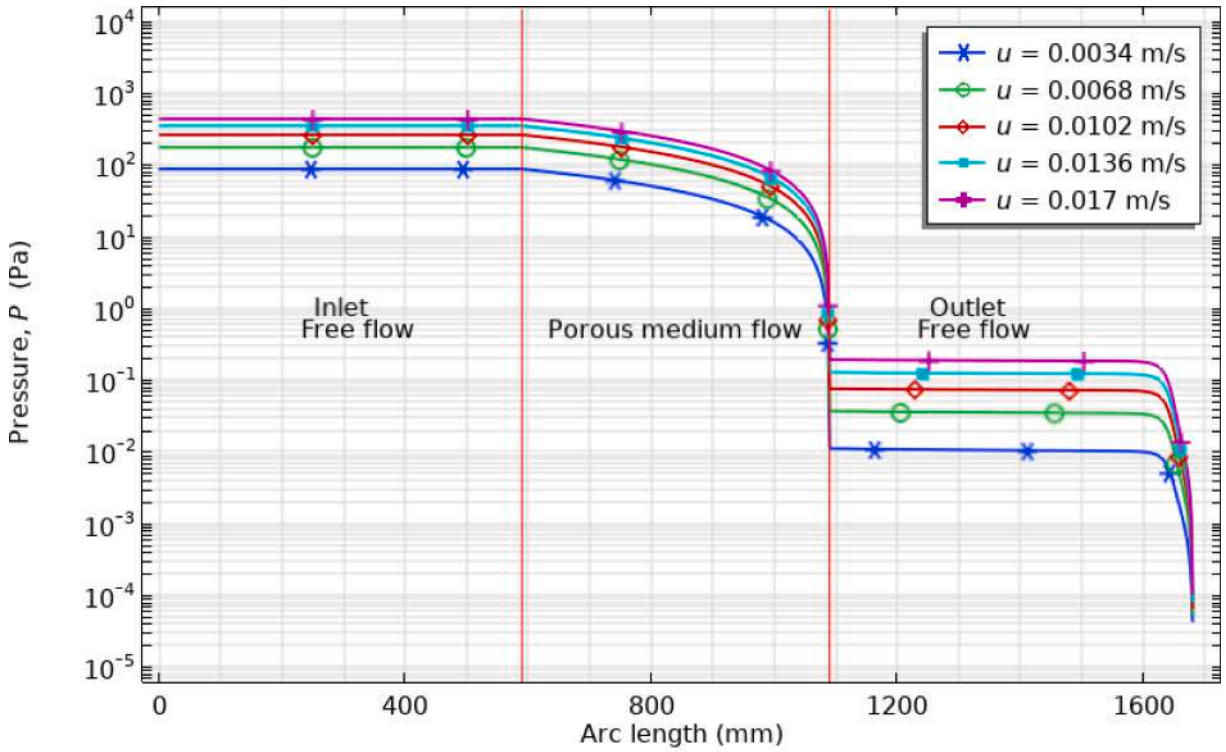

(d) $d_p = 2.500$ mm

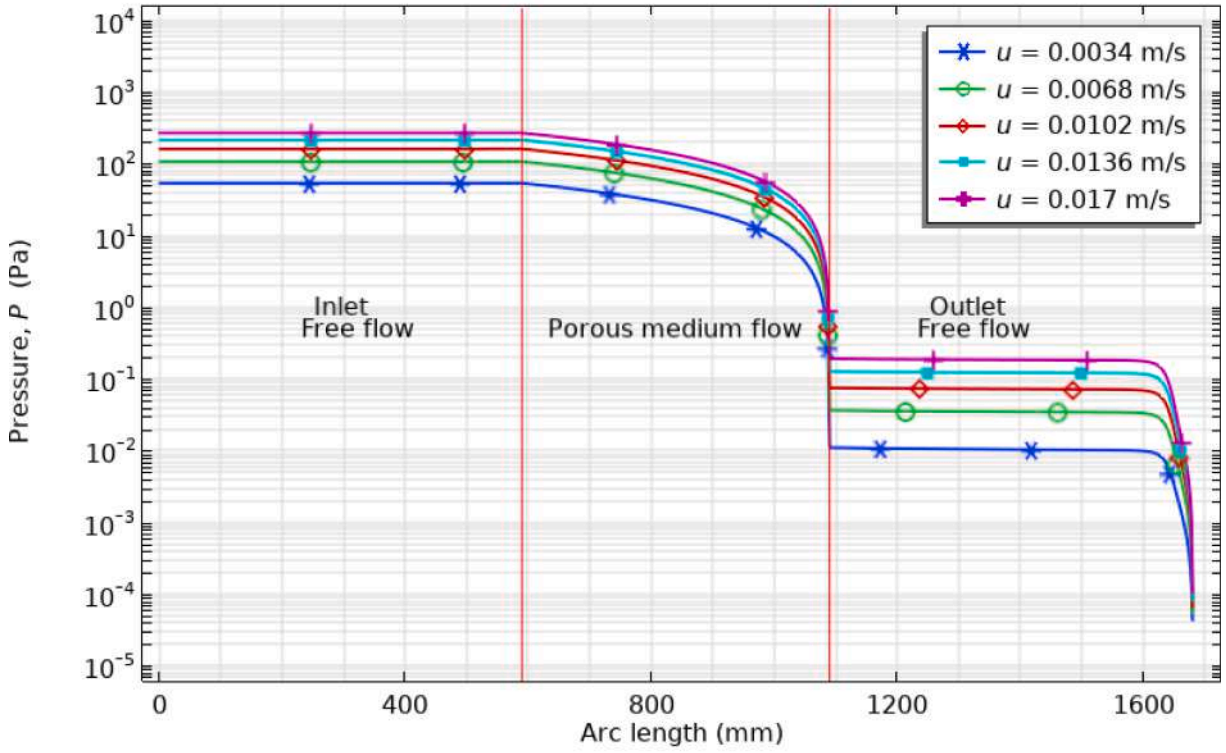

(e) $d_p = 3.170$ mm.

Fig. 7. (*continued*).

Appendix A

The fully coupled solver is used in COMSOL Multiphysics. The solver starts with an initial guess and applies Newton-Raphson iterations until the solution has converged as shown in the following block diagram of Fig. A1:

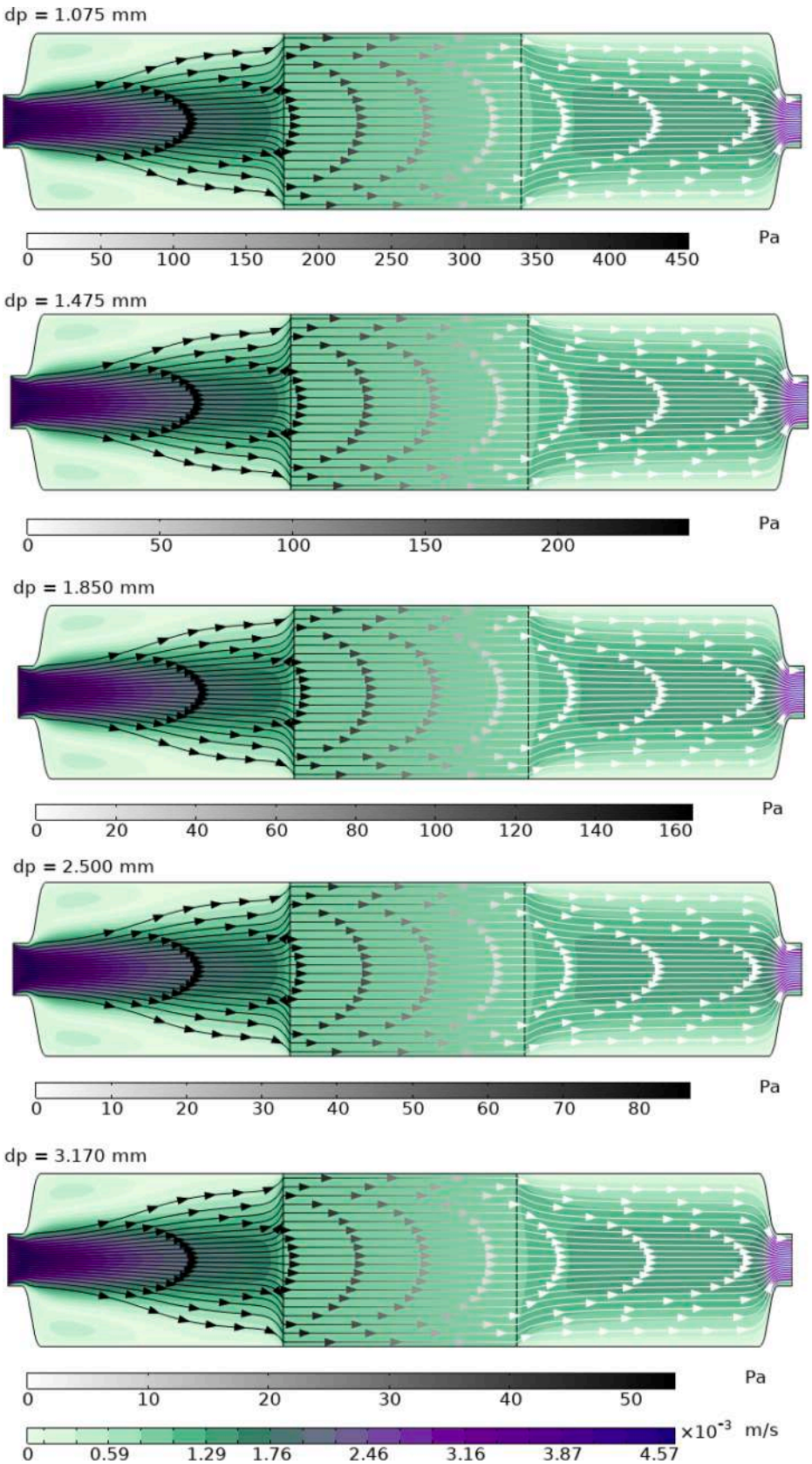

Fig. 8. Velocity contour at 0.001 m/s inlet porous medium velocity.

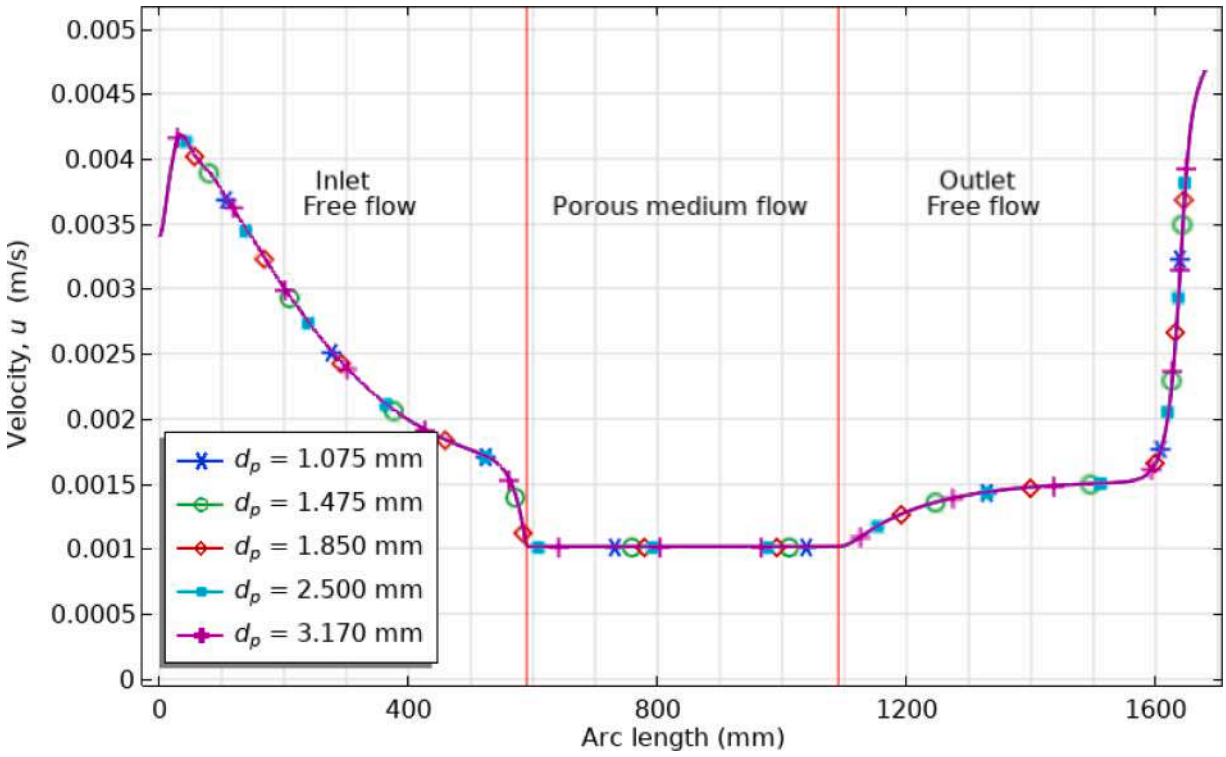

Fig. 9. Velocity profile under 0.001 m/s inlet porous medium velocity.

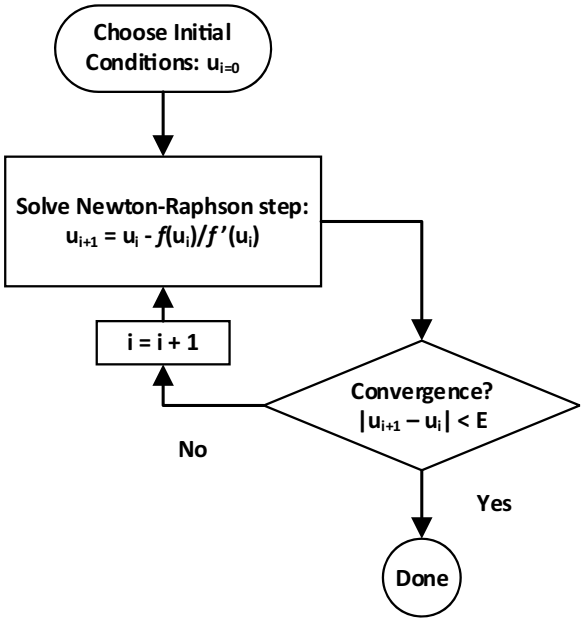

Fig. A1. The solution procedure of COMSOL multiphysics.

When solving such a problem, you will get a convergence plot (see Fig. A2), which shows the error estimate decreasing between Newton-Raphson iterations. Ideally, the error should go down monotonically if it does converge.

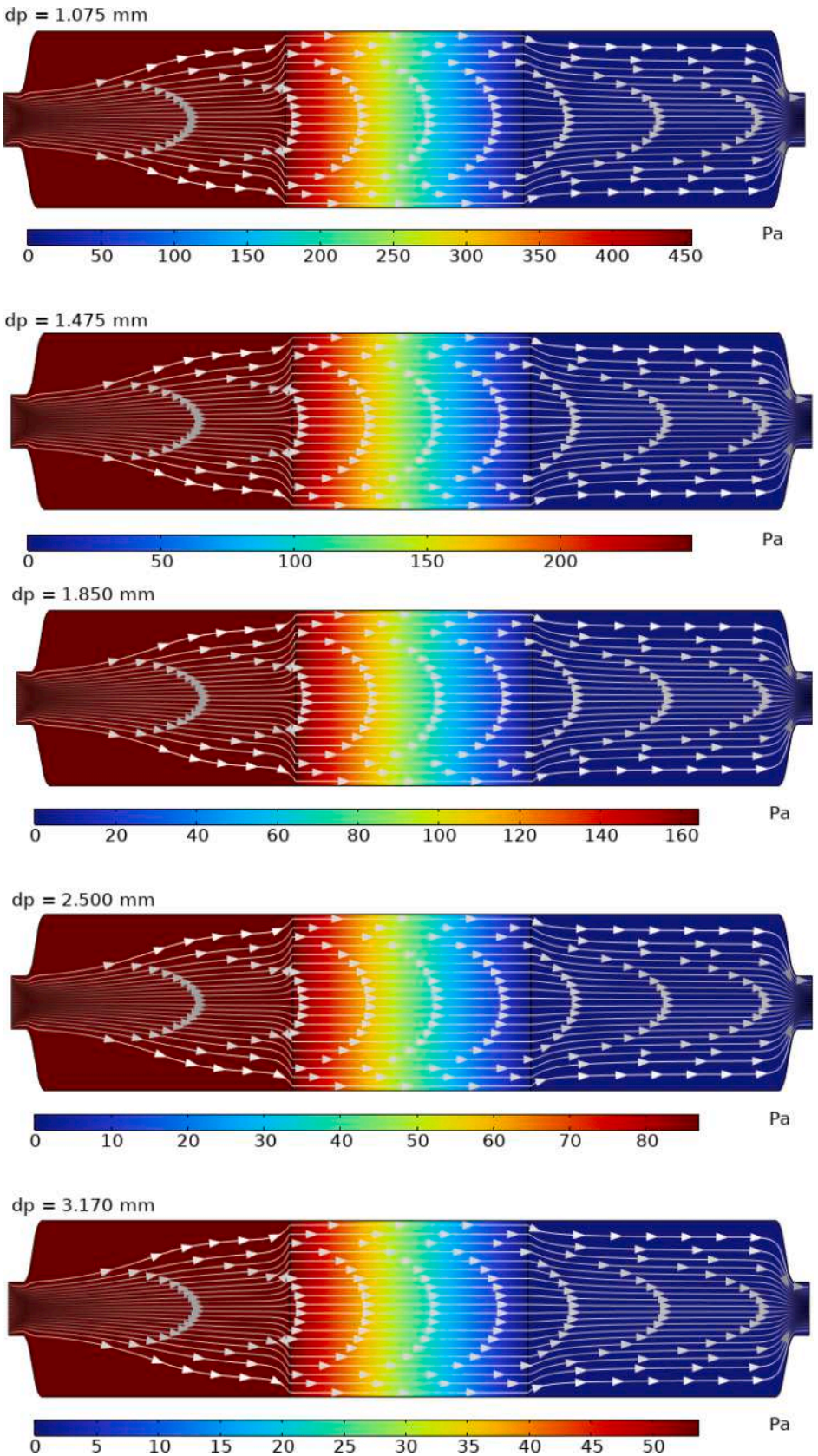

Fig. 10. Pressure contour at 0.001 m/s inlet porous medium velocity.

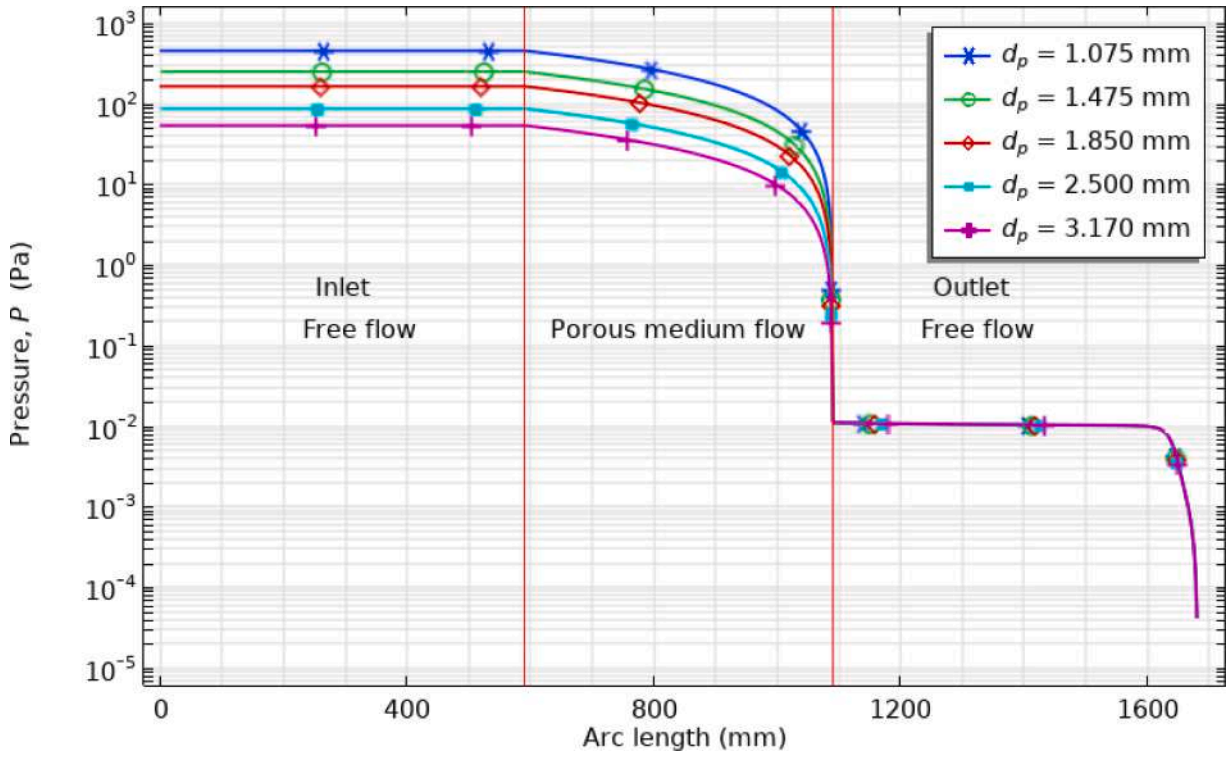

Fig. 11. Local pressure under 0.001 m/s inlet porous medium velocity.

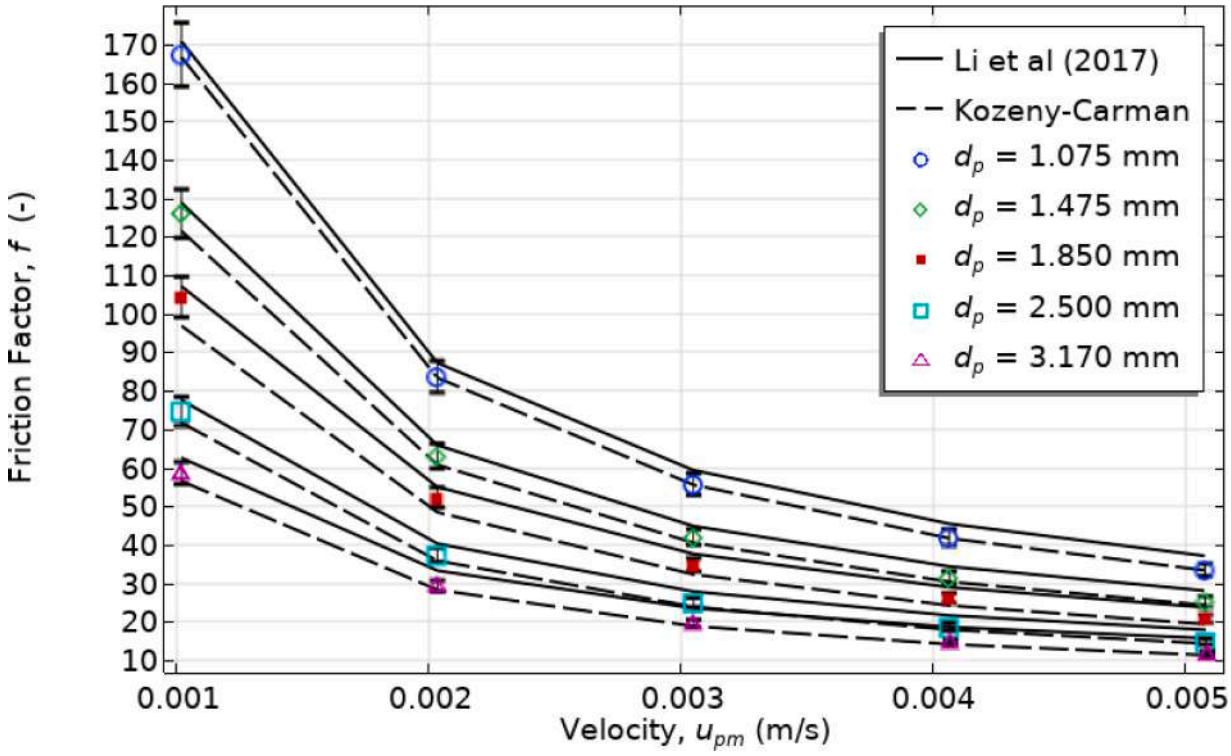

Fig. 12. Characteristics of friction factors at various inlet velocities for each particle size.

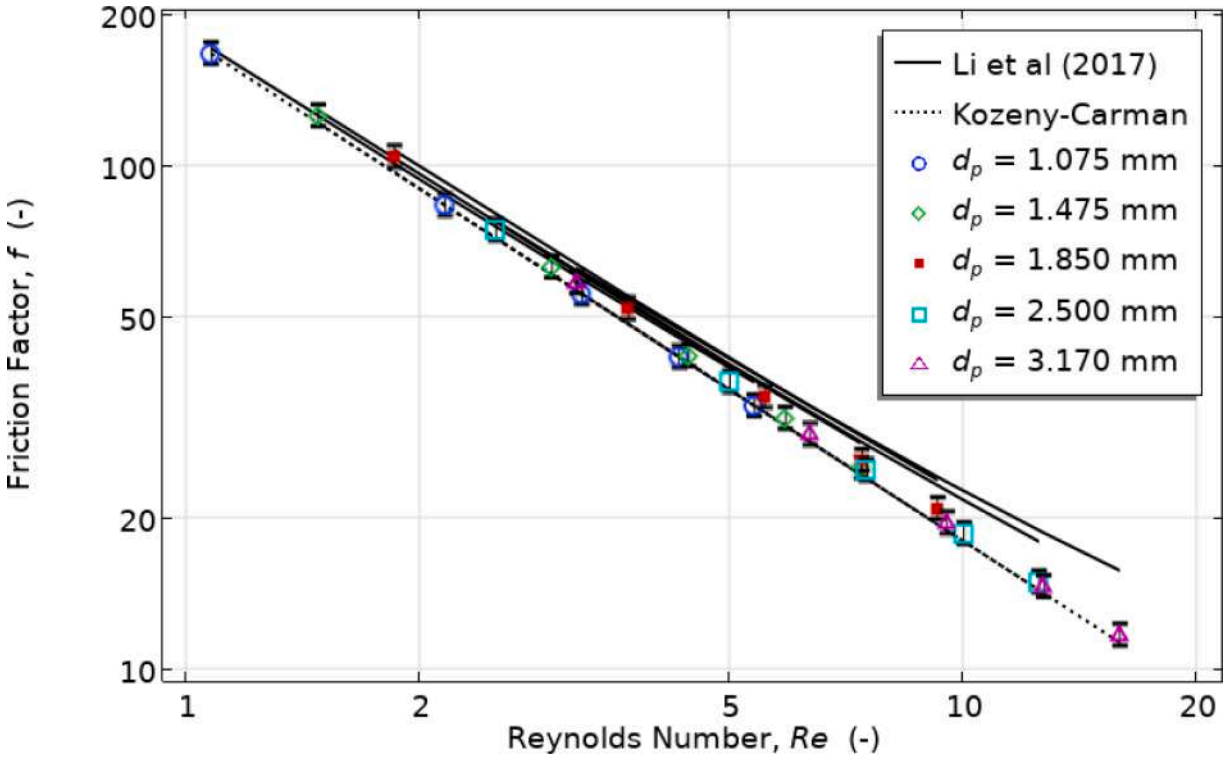

Fig. 13. Characteristics of friction factors at various Reynolds numbers for each particle size.

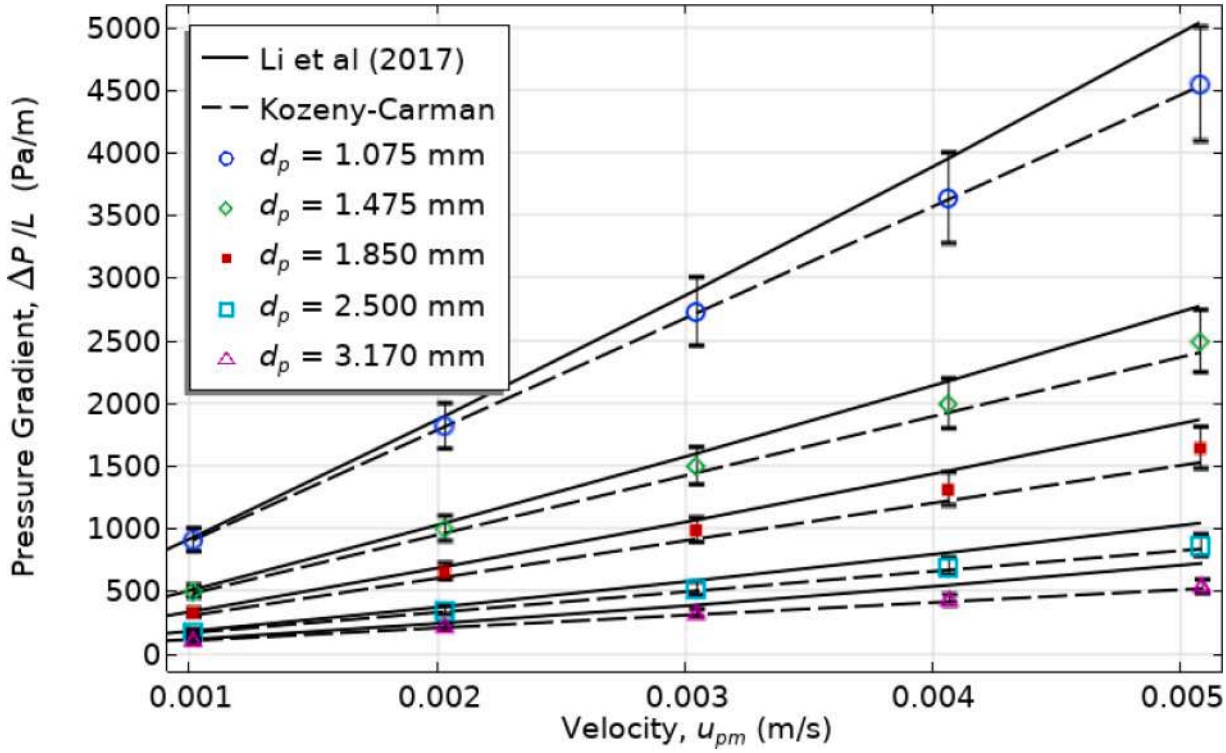

Fig. 14. Characteristics of pressure gradient at various inlet velocities for each particle size.

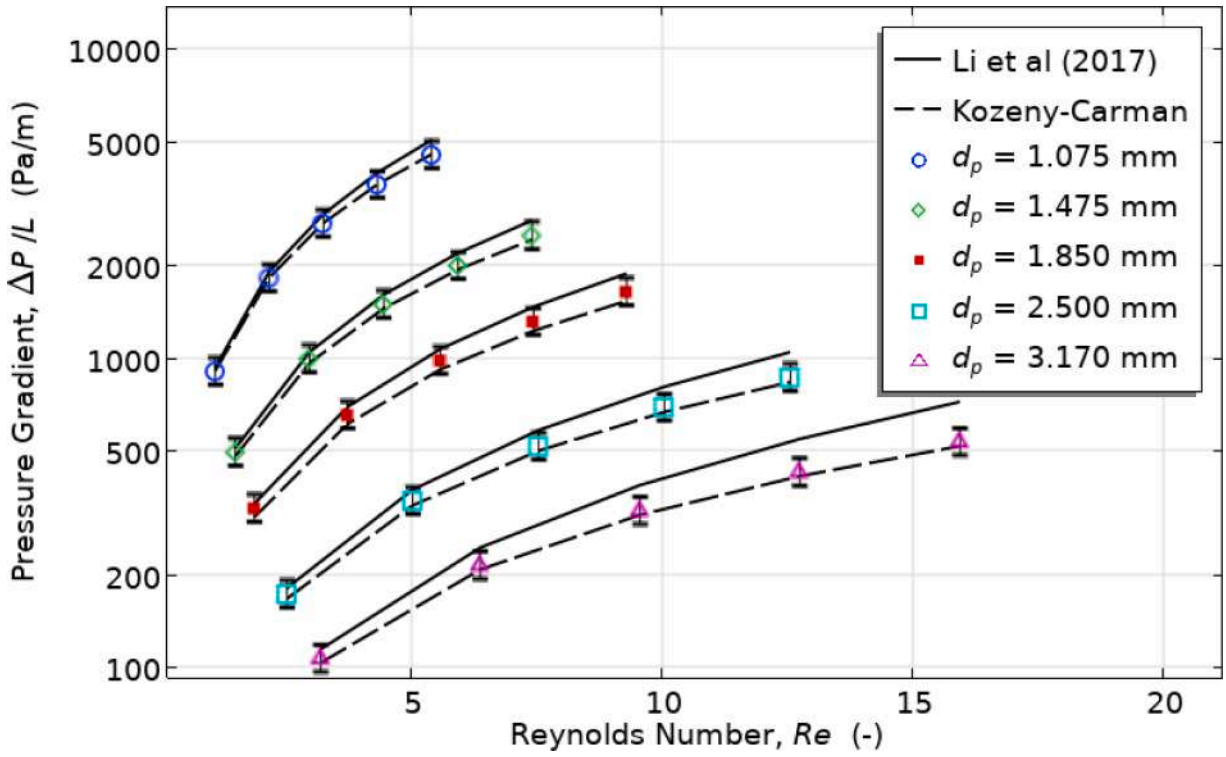

Fig. 15. Characteristics of pressure gradient at various Reynolds numbers for each particle size.

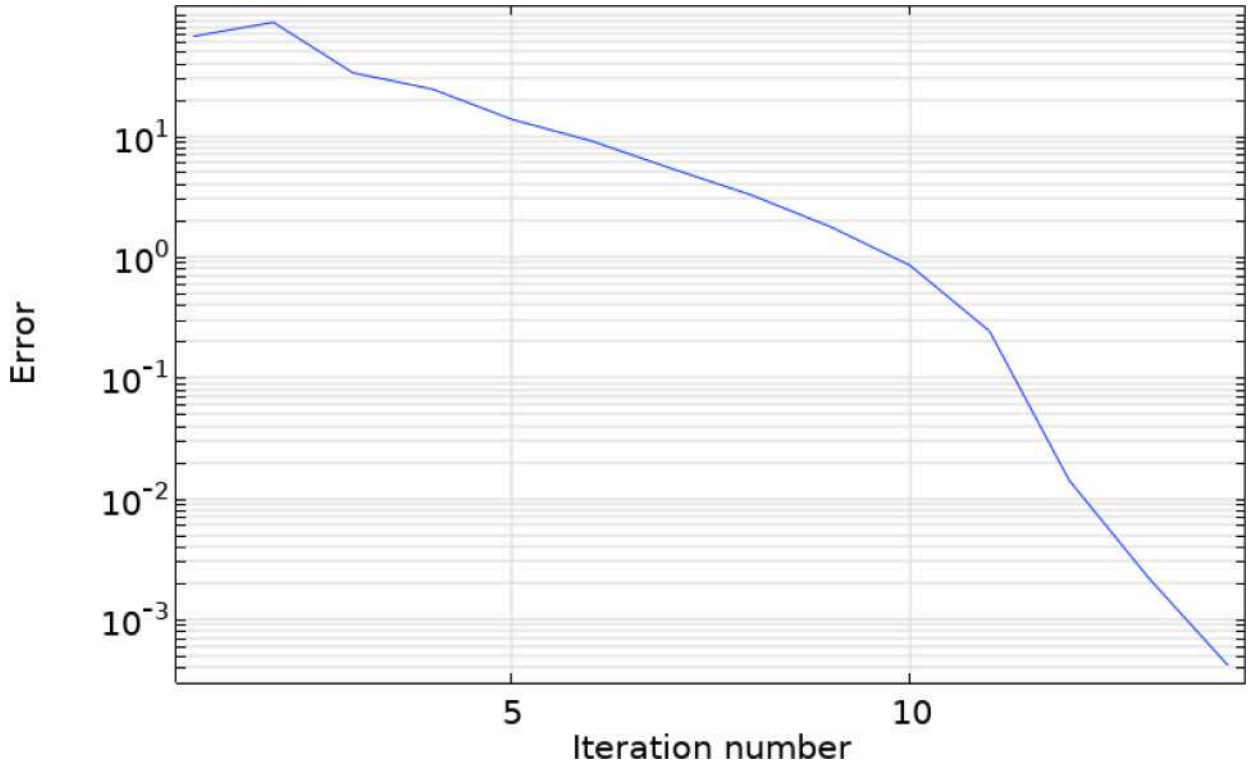

Fig. A2. Convergence plot for inlet velocity of 10 m/s with the fine mesh size.

The following block diagram of Fig. A3 illustrates the steps for mesh convergence analysis in COMSOL multiphysics.

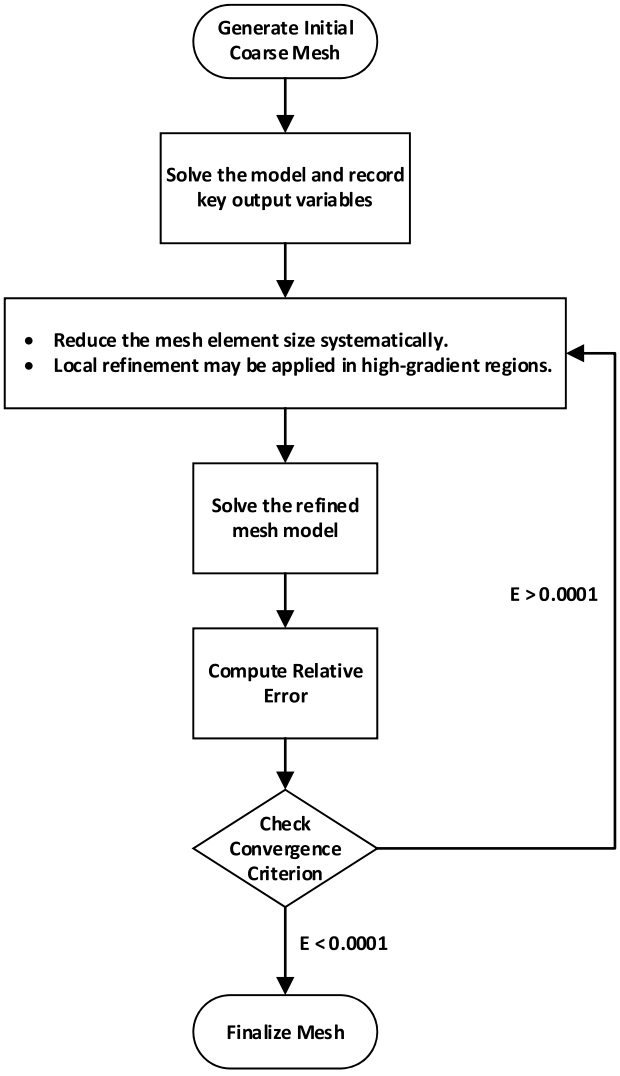

Fig. A3. Steps for mesh convergence analysis in COMSOL multiphysics.

Data availability

Data will be made available on request.

References

[1] D.A. Nield, A. Bejan, Convection in Porous Media, 3, springer, New York, 2006.
[2] Z. Ullah, Mohamed Ahmed Said, M.D. Alsulami, Saleh Al Arni, Nidal H.E. Eljaneid, Ali Hakami, Nidhal Ben Khedher, Thermal radiation and soret/dufour effects on amplitude and oscillating frequency of darcian mixed convective heat and mass rate of nanofluid along porous plate, Case Stud. Therm. Eng. 59 (2024) 104562, https://doi.org/10.1016/j.csite.2024.104562.
[3] Bai Mbye Cham, Shams-ul Islam, Zia-ul Islam, Numerical study on natural convection in a saturated non Darcian porous medium under radiation and entropy generation effects, Appl. Therm. Eng. 250 (2024) 123491, https://doi.org/10.1016/j.applthermaleng.2024.123491.
[4] N. Vishnu Ganesh, Qasem M. Al-Mdallal, R. Kalaivanan, K. Reena, Arrhenius kinetics driven nonlinear mixed convection flow of Casson liquid over a stretching surface in a Darcian porous medium, Heliyon. 9 (6) (2023) e16135, https://doi.org/10.1016/j.heliyon.2023.e16135.
[5] S. Arbabi, M. Sahimi, The transition from Darcy to nonlinear flow in heterogeneous porous media: I—single-phase flow, Transp. Porous Med. 151 (2024) 795–812, https://doi.org/10.1007/s11242-024-02070-3.
[6] A. Atangana, Fractional Operators with Constant and Variable Order with Application to Geo-Hydrology, Academic Press, 2017.
[7] R.M. Fand, B.Y.Y. Kim, A.C.C. Lam, R.T. Phan, Resistance to the flow of fluids through simple and complex porous media whose matrices are composed of randomly packed spheres, J. Fluids Eng. 109 (1987) 268–273.
[8] I. Kececioglu, Y. Jiang, Flow through porous media of packed spheres saturated with water, J. Fluids Eng. 116 (1994) 164–170.
[9] D. Seguin, A. Montillet, J. Comiti, F. Huet, Experimental characterization of flow regimes in various porous media—II: transition to turbulent regime, Chem. Eng. Sci. 53 (1998) 3897–3909, b.
[10] J. Bear, Dynamics of Fluids in Porous Media, Dovers, New York, 1972.
[11] M. Kaviany, Principles of Heat Transfer in Porous Media, 2nd edn., Springer, New York, 1995. Kececioglu, I., Jiang, Y.: Flow through porous media of packed spheres saturated with water. J. Fluids Eng. 116, 164–170 (1994).
[12] D.A. Nield, A. Bejan, Convection in Porous Media, 2nd edn., Springer, New York, 1999. Panfilov, M., Fourar, M.: Physical splitting of non-linear effects in high-velocity stable flow through porous media. Adv. Water Res. 331, 41–48 (2006).
[13] I. Macdonald, M. El-Sayed, K. Mow, F. Dullien, Flow through porous media-the Ergun equation revisited, Ind. Eng. Chem. Fundam. 18 (1979) 199–208.
[14] H.F. Burcharth, O.H. Andersen, On the one-dimensional steady and unsteady porous flow equations, Coast. Eng. 24 (1995) 233–257.
[15] K.G. Allen, T.W. von Backstroem, D.G. Kroeger, Packed bed pressure drop dependence on particle shape, size distribution, packing arrangement and roughness, Powder. Technol. 246 (2013) 590–600.
[16] P.C. Carman, Fluid flow through granular beds, Trans. Inst. Chem. Eng. 15 (1937) 150–166.
[17] S. Ergun, Fluid flow through packed columns, Chem. Eng. Prog. 48 (1952) 89–94.
[18] J. Ward, Turbulent flow in porous media, J. Hydraul. Div. 90 (1964) 1–12.
[19] S. Irmay, Theoretical models of flow through porous media, in: Proceedings of the International Symposium on Transport of Water in Porous Media, Paris, France 29, 1964, pp. 37–43.

[20] G. Kovacs, Seepage Hydraulics, Elsevier Scientific Publishing Company, Amsterdam, The Netherlands, 1981. ISBN 0-444-99755-5.
[21] R.M. Fand, R. Thinakaran, The influence of the wall on flow through pipes packed with spheres, J. Fluids Eng. 112 (1990) 84–88.
[22] R.H. Kadlec, S. Wallace, Treatment Wetlands, 2nd ed., CRC Press, Boca Raton, FL, USA, 2008, pp. 43–44. ISBN 978-1-56670-526-4.
[23] M.G. Sidiropoulou, K.N. Moutsopoulos, V.A. Tsihrintzis, Determination of forchheimer equation coefficients a and b, Hydrol. Process. 21 (2007) 534–554.
[24] F. Siddiqui, Y. Soliman, W. House, A. Ibragimov, Pre-Darcy flow revisited under experimental investigation, J Anal Sci. Technol. 7 (2) (2016) 1–9, https://doi.org/10.1186/s40543-015-00812.
[25] X. Wang, J. Sheng, Discussion of liquid threshold pressure gradient, Petroleum 3 (2017) 232–236.
[26] M. Sedghi-Asl, H. Rahimi, Adoption of Manning's equation to 1D non-Darcy flow problems, J. Hydraul. Res. 49 (6) (2011) 814–817.
[27] R.E. Hayes, A. Afacan, B. Boulanger, An equation-of-motion for an incompressible newtonian fluid in a packed-bed, Transp. Porous Media 18 (1995) 185–198.
[28] R.P. Dias, C.S. Fernandes, J.A. Teixeira, M. Mota, A. Yelshin, Permeability analysis in bisized porous media: wall effect between particles of different size, J. Hydrol. 349 (2008) 470–474.
[29] F.-Y. Tian, L.-F. Huang, L.-W. Fan, H.-L. Qian, Z.-T Yu, Wall effects on the pressure drop in packed beds of irregularly shaped sintered ore particles, Powder. Technol. 301 (2016) 1284–1293.
[30] R.H. Kadlec, S. Wallace, Treatment Wetlands, 2nd ed., CRC Press, Boca Raton, FL, USA, 2008, pp. 43–44.
[31] J. Soni, N. Islam, P. Basak, An experimental evaluation of non-darcian flow in porous media, J. Hydrol. 38 (1978) 231–241.
[32] K. Huang, J.W. Wan, C.X. Chen, L.Q. He, W.B. Mei, M.Y. Zhang, Experimental investigation on water flow in cubic arrays of spheres, J. Hydrol. 492 (2013) 61–68.
[33] M. Sedghi-Asl, H. Rahimi, R. Salehi, Non-darcy flow of water through a packed column test, Transp. Porous Media 101 (2014) 215–227.
[34] R.F. Benenati, C.B. Brosilow, Void fraction distribution in beds of spheres, Am. Inst. Chem. Eng. 8 (1962) 359–361.
[35] G.S. Beavers, E.M. Sparrow, D.E. Rodenz, Influence of bed size on the flow characteristics and porosity of randomly packed beds of spheres, J. Appl. Mech. 40 (1973) 655–660.
[36] Z. Li, J. Wan, K. Huang, W. Chang, Y. He, Effects of particle diameter on flow characteristics in sand columns, Int. J. Heat Mass Transf. 104 (2017) 533–536.
[37] M.H. Abed, H.A. Al-Asadi, A. Oleiwi, S.A. Kadhim, M. Al-Yasiri, A.M. Alsayah, et al., Improving building energy efficiency through ventilated hollow core slab systems, Case Stud. Therm. Eng. 60 (2024) 104793, https://doi.org/10.1016/j.csite.2024.104793.
[38] S.A. Kadhim, K.A. Hammoodi, M.J. Alshukri, I. Omle, K.K.A. Hussein, A.F. Khalaf, et al., Enhancing the melting rate of RT42 paraffin wax in a square cell with varied copper fin lengths and orientations: a numerical simulation, Int. J. Thermofluids 24 (2024) 100877, https://doi.org/10.1016/j.ijft.2024.100877.
[39] Z. Li, J. Wan, K. Huang, W. Chang, Y. He, Effects of particle diameter on flow characteristics in sand columns, Int. J. Heat Mass Transf. 104 (2017), https://doi.org/10.1016/j.ijheatmasstransfer.2016.08.085.
[40] K.A. Hammoodi, I.A. Abdulghafor, S.A. Kadhim, A. Elsheikh, D.R. Nayyaf, A mohsin Alsayah, et al., Effect of air layer on PCMs melting process inside a spherical container: a numerical investigation, Results. Eng. 24 (2024) 103088, https://doi.org/10.1016/j.rineng.2024.103088.
[41] P.C. Carman, Fluid flow through granular beds, Chem. Eng. Res. Des. 75 (1 SUPPL) (1997), https://doi.org/10.1016/s0263-8762(97)80003-2.
[42] P.C. Carman, Flow of Gases Through Porous Media, Butterworths, London, 1956.
[43] P. Kundu, V. Kumar, I.M. Mishra, Experimental and numerical investigation of fluid flow hydrodynamics in porous media: characterization of pre-Darcy, Darcy and non-Darcy flow regimes, Powder. Technol. 303 (2016), https://doi.org/10.1016/j.powtec.2016.09.037.
[44] S.A. Kadhim, K.A. Hammoodi, A.H. Askar, F.L. Rashid, H.A. Abdul Wahhab, Feasibility review of using copper oxide nanofluid to improve heat transfer in the double-tube heat exchanger, Results. Eng. 24 (2024) 103227, https://doi.org/10.1016/j.rineng.2024.103227.